Discovery of Novel Quinoline-Chalcone Derivatives as Potent Anti-tumor Agents with Microtubule Polymerization Inhibitory Activity

Wenlong Li,[†] Feijie Xu,[†] Wen Shuai,[†] Honghao Sun,[†] Hong Yao,[†] Cong Ma,[‡] Shengtao Xu,[,†] Hequan Yao,[†] Zheying Zhu,[#] Dong-Hua Yang,[§] Zhe-Sheng Chen,[§] Jinyi Xu [*,†]*

[†]State Key Laboratory of Natural Medicines and Department of Medicinal Chemistry, China Pharmaceutical University, 24 Tong Jia Xiang, Nanjing 210009, P. R. China

[‡]State Key Laboratory of Chemical Biology and Drug Discovery, and Department of Applied Biology and Chemical Technology, The Hong Kong Polytechnic University, Kowloon, Hong Kong

[#]Division of Molecular Therapeutics & Formulation, School of Pharmacy, The University of Nottingham, University Park Campus, Nottingham NG7 2RD, U. K.

[§]College of Pharmacy and Health Sciences, St. John's University, 8000 Utopia Parkway, Queens, New York 11439, United States

ABSTRACT

A series of novel quinoline-chalcone derivatives were designed, synthesized and evaluated for their antiproliferative activity. Among them, compound **24d** exhibited the most potent activity with IC_{50} values ranging from 0.009 to 0.016 μM in a panel of cancer cell lines. Compound **24d** also displayed a good safety profile with LD_{50} value of 665.62 mg/kg by intravenous injection, and its hydrochloride salt **24d-HCl**

significantly inhibited tumor growth in H22 xenograft models without observable toxic effects, which was more potent than that of CA-4. Mechanism studies demonstrated that **24d** bound to the colchicine site of tubulin, arrested cell cycle at the G2/M phase, induced apoptosis, depolarized mitochondria and induced reactive oxidative stress (ROS) generation in K562 cells. Moreover, **24d** has potent *in vitro* anti-metastasis, *in vitro* and *in vivo* anti-vascular activities. Collectively, our findings suggest that **24d** deserves to be further investigated as a potent and safe anti-tumor agent for cancer therapy.

INTRODUCTION

Microtubules provides a dynamic scaffold for maintenance of cell structure, protein trafficking, chromosomal segregation, and mitosis.[1] They are long, hollow structures that are mainly composed of α- and β-tubulin dimers. [2-4] Microtubule-targeting agents (MTAs) including microtubule stabilizers or destabilizers can interfere with microtubule dynamics, leading to mitotic blockade and cell apoptosis.[5] In recent decades, MTAs that bind to the colchicine site have been attracting the interest of medicinal chemists because of their advantages over other site binders; these MTAs have simpler structures, improved aqueous solubility, broad therapeutic index, and reduced multidrug resistance (MDR) effects as comparing with other site binders.[6-12] Notably, colchicine binding site inhibitors (CBSIs) can induce morphological changes in endothelial cells, thus provoking a rapid disrupt of existing tumor vasculature, and thus are commonly designated as vascular disrupting agents (VDAs).[13, 14]

Chalcones that bear an α, β-unsaturated ketone moiety represents a key structural

motif in the plethora of biologically active molecules including synthetic and natural products. They have shown a broad range of biological activities such as antioxidant, antibacterial, antifungal, anti-HIV, anti-leishmanial, antimalarial, anti-inflammatory, and anticancer properties.[15] In the development process of CBSIs, the α, β-unsaturated ketone moiety of chalcones was recognized as a privileged structure.[16-20] Representative anti-tubulin chalcones, presented as compounds **1** and **2** (Figure 1a), showed remarkable antiproliferative activities.[21] The more preferential *s-trans* conformation adopted by **2**, which could interact with tubulin more easily, led to more potent cytotoxicity than **1**. Another chalcone compound reported by Li's group was compound **3**, which exhibited excellent antipoliferative activity with IC_{50} values ranging from 3 to 9 nM against a panel of cancer cell lines.[22] Our previous work on the modification of compound **1** also led to a novel chalcone analog **4**, which displayed both potent anti-vascular and anti-tumor activities.[23]

Nitrogenous molecules, such as pyridines and quinolines, have numerous advantages over other non-nitrogenous molecules. The introduction of nitrogen atom greatly improves the basicity of molecules due to its basic characteristic, and nitrogen atom may form a strong hydrogen bond with the targets. Another important property is the polarity which can be used as a mean of reducing the lipophilic character, improving water solubility and oral absorption.[24] The quinoline motif is frequently found in natural alkaloids that exhibit a wide range of biological activities. The quinoline ring system-containing drugs, such as quinine, chloroquine, mefloquine and amodiaquine, are used as efficient treatments of malaria.[25] Quinoline analogs also

exhibit anticancer activities with different mechanisms, including alkylating agents, tyrosine kinase inhibitors and tubulin inhibitors.[26]

Considering the poor aqueous solubility that impeded the clinical development of some CBSIs,[27] incorporation of nitrogenous heterocycles, which could be salified with acids, may improve water solubility. Some examples of tubulin inhibitors bearing a quinoline skeleton are listed in Figure 1b, such as compounds **5**[28], **6**[29] and **7** - **11**[30-34]. Recently, the work performed by Alami et al. also proved that a quinoline ring as shown in compound **12** can replace the 3,4,5-trimethoxyphenyl moiety and provide compounds with more potent activities.[35] Their docking studies predicted that the *N*-1 atom of quinoline formed a hydrogen bond with the critical residue Cys 241, which was further supported by the later disclosed crystal structure of tubulin in complex with **11**.[34] Thus, the quinoline moiety might be a surrogate of the 3,4,5-trimethoxyphenyl moiety when binding to the colchicine site.

Our group has concentrated on discovering and developing novel anticancer agents targeting the tubulin-microtubule system.[23, 36, 37] In our continuing works on the structural modification of the parent compound **1** around the 3,4,5-trimethoxyphenyl, which led to the discovery of a series of novel quinoline-chalcone derivatives (Figure 2). Meanwhile, given previous studies showed that the indole moiety was an alternative structure of the isovanillic ring.[38, 39] Thus, new quinoline-chalcones that contain an indole moiety were also designed and synthesized. Herein, we would like to report their synthesis and anti-tumor activities *in vitro* and *in vivo*. In addition, the underlying cytotoxic mechanisms of the representative compound **24d** are also

elucidated.

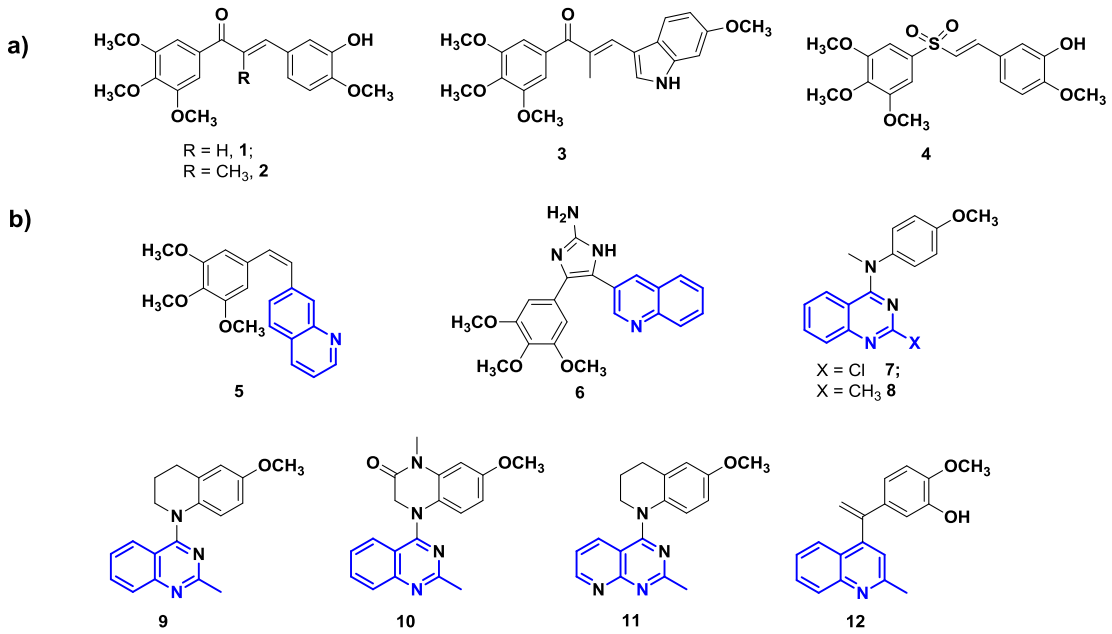

Figure 1. a) Representative anti-tubulin chalcones or chalcone analogs; b) Tubulin inhibitors bearing quinoline and quinazoline skeletons.

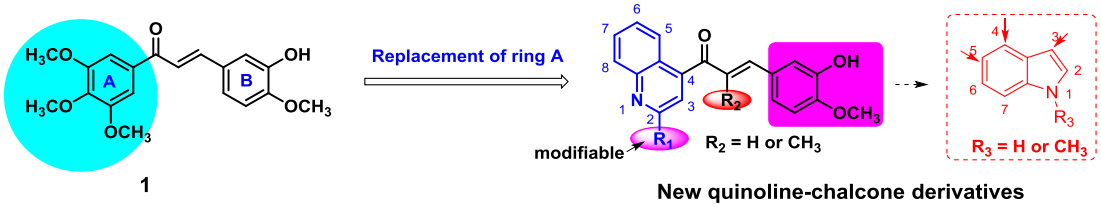

Figure 2. Design strategy of novel quinoline-chalcone derivatives.

RESULTS AND DISCUSSION

Chemical Synthesis. In Alami's previous work,[35] the effects of different substitutions at the C-2 position of quinoline were investigated in detail with a methyl group being the most active. Thus, 2-methylquinoline was first chosen to replace the 3,4,5-trimethoxyphenyl moiety of compound **1**. The synthetic route of key

intermediates acetylquinoline **16** and propionylquinoline **21** was outlined in Scheme 1. 2-Methylquinoline-4-carboxylic acid (**14**) was prepared by refluxing the commercially available material isatin (**13**) with acetone under basic conditions, which was further converted into Weinreb amide **15**, and **15** reacted with methylmagnesium bromide (CH_3MgBr) to obtain acetylquinoline **16** in high yields. Disappointingly, this method was not applicable for the synthesis of propionylquinoline **21** due to the overreaction of **21** with ethylmagnesium bromide (C_2H_5MgBr) resulting in a great decreased yield. Thus, we attempted a tedious but effective route to synthesize **21**. 2-Methylquinoline-4-carbaldehyde (**19**) was prepared by the oxidation of **18** according to the previous report [40]. Then, **19** underwent nucleophilic attack by CH_3CH_2MgBr to obtain **20**, which was subsequently oxidized to produce the propionylquinoline **21**.

The designed target compounds **24a-o** containing a 2-methylquinoline moiety were synthesized using acetylquinoline **16** or propionylquinoline **21** with various commercially available aldehydes via aldol condensation reactions (Scheme 2). Compound **24a** and **24b** bearing amino groups were synthesized using 3-nitro-4-methoxybenzaldehyde (**22**) in the condensation steps, after which the nitro group was reduced to amino group to afford **24a** and **24b**. Similarly, the MEM protective group was used to synthesize **24c** and **24d** bearing an isovanillic ring. The aldol reactions of **16** or **21** with various benzaldehydes or indole formaldehydes provided the target compounds **24e-o**.

Scheme 1. The synthetic route of key intermediates **16** and **21**[a].

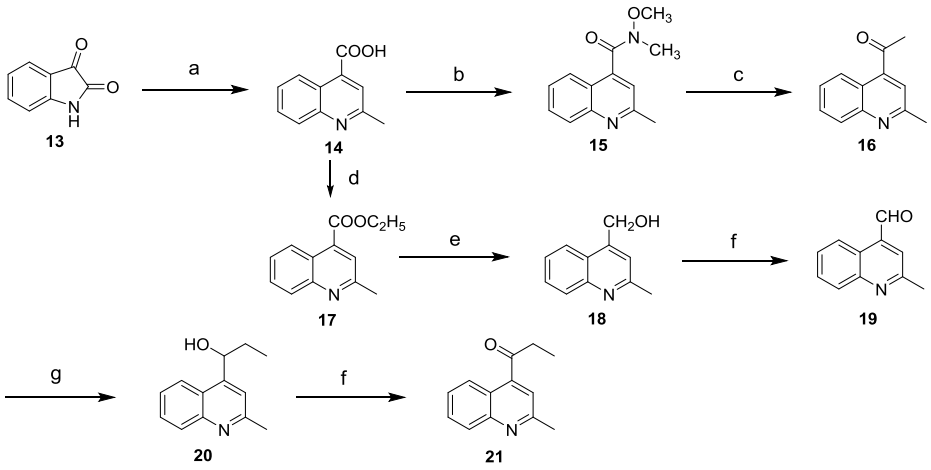

[a]Reagents and conditions: (a) 85% KOH aqueous, acetone, 50 ℃, 24 h, 82.3%; (b) CH_3NHOCH_3-HCl, EDCI, HOBt, DMAP(cat.), DCM, rt, 2 h, 83.1%; (c) CH_3MgBr, THF, 0 ℃ to rt, 2 h, 84.0%; (d) i) oxalyl chloride, DMF (cat.), DCM; ii) C_2H_5OH; 72.2% over two steps; (e) $NaBH_4$, CH_3OH; 0 ℃ to rt, 4 h, 63.5%; (f) Dess-Martin reagent, DCM; 2 h, rt, 65.1-80.0%; (g) C_2H_5MgBr, THF, 0 ℃ to rt, 2 h, 74.1%.

Subsequently, compounds bearing a quinoline moiety with varying substitutions at the C-2 position were designed and synthesized. Compounds **29a** and **29b** with hydroxymethyl and formyl groups at the C-2 position of the quinoline ring were synthesized as shown in Scheme 3. Intermediate **28** was prepared by a rearrangement reaction of quinoline-*N*-oxide **27**, and a further aldol reaction with MEM protected isovanillin **25** led to **29a**, which was oxidized to formyl substituted target compound **29b**.

Scheme 2. The synthetic route of key intermediates **24a-o**[a].

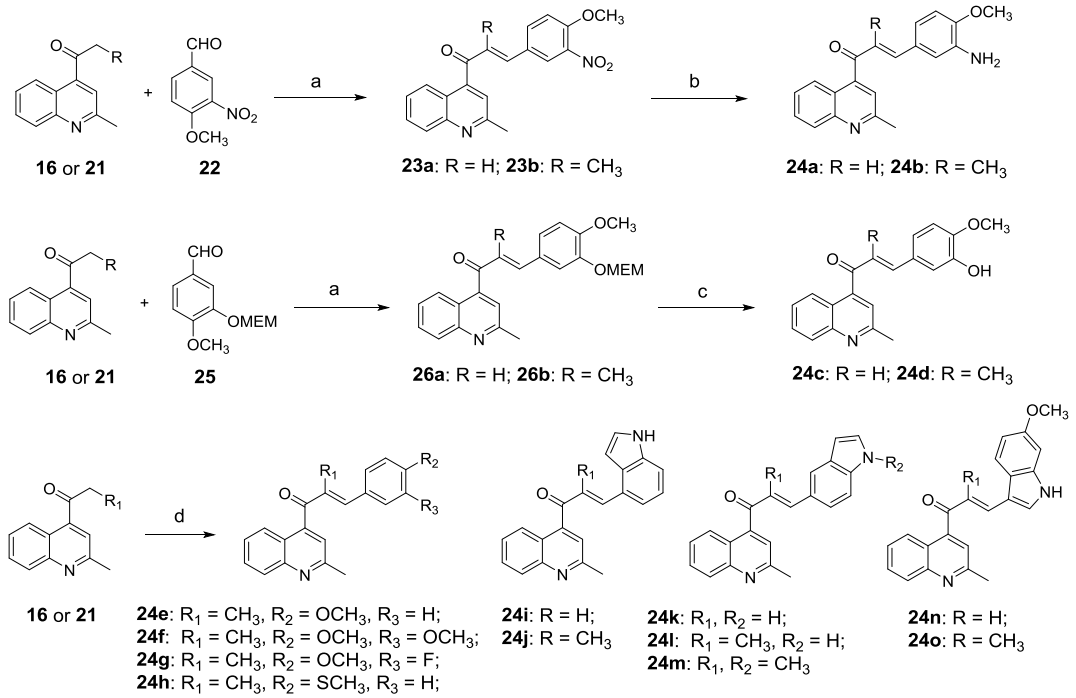

[a]Reagents and conditions: (a) NaOH, EtOH, rt, 30 min, moderate yields; (b) Fe, AcOH, EtOH, reflux; 62.5-73.2%; (c) 10% HCl, EtOH, 30 min, 85-95%; (d) different benzaldehydes, NaOH, EtOH, rt, 30 min, moderate yields or different indole formaldehydes, piperidine, EtOH, reflux, moderate yields.

Scheme 3. The synthetic route of key intermediates **29a** and **29b**[a].

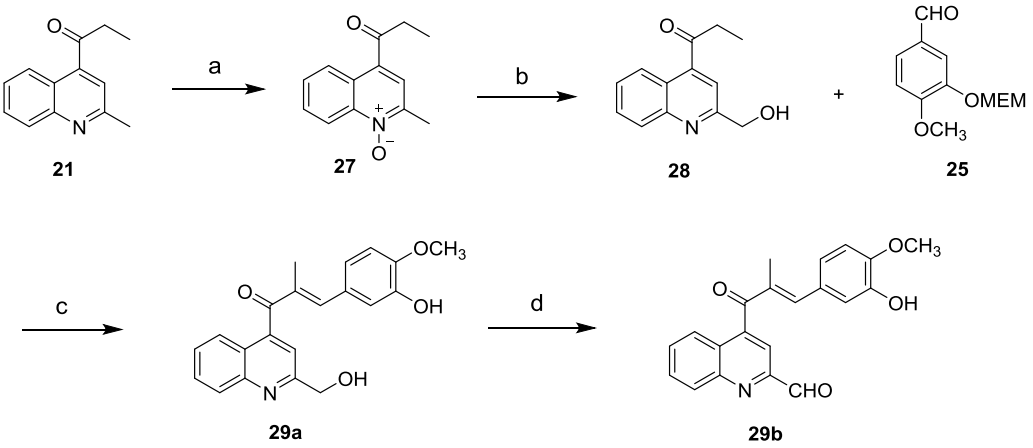

[a]Reagents and conditions: (a) *m*-CPBA, DCM, 2 h, rt, 89.0%; (b) i) Ac_2O, reflux, 2 h, 86.2%; ii) 10% NaOH aqueous, CH_3OH, 30 min, 88.2%; (c) i) NaOH, EtOH, rt, 30 min; ii) 10% HCl, EtOH, reflux, 30 min; 43.7%; (d) IBX, DMSO, rt, 30 min, 74.9%.

Chloro-substituted propionylquinoline **36** was prepared as shown in Scheme 4. Intermediate **30** was prepared by refluxing isatin **13** with malonic acid in glacial acetic acid, following a chlorination by $POCl_3$ leading to 2-chloroquinoline-4-carboxylic acid (**31**), which was converted to propionylquinoline **36** according to the synthesis method of intermediate **21**. Propionylquinolines **37a-c** were prepared by nucleophilic reactions of **36** with secondary amines. Because primary amines can react with the ketone group of **36** to form Schiff bases, we used **35**, the precursor of **36**, to react with various primary amines followed by oxidations by IBX to afford intermediates **39a-d**. Cyano containing propionylquinoline **40** was prepared by a Pd-catalyzed coupling reaction of **36** with $Zn(CN)_2$, and a methoxy group was introduced by a nucleophilic reaction of **36** with $NaOCH_3$ to give intermediate **41**. In our attempts to introduce a mesyl group to the C-2 position of quinoline, the lactam **42** was occasionally obtained, which was then used for the next derivation to synthesize compound 29m. Propionylquinoline **45** was prepared using commercially available quinolone-4-carbaldehyde (**43**) as the starting material.

Scheme 4. The synthetic route of key intermediates [a].

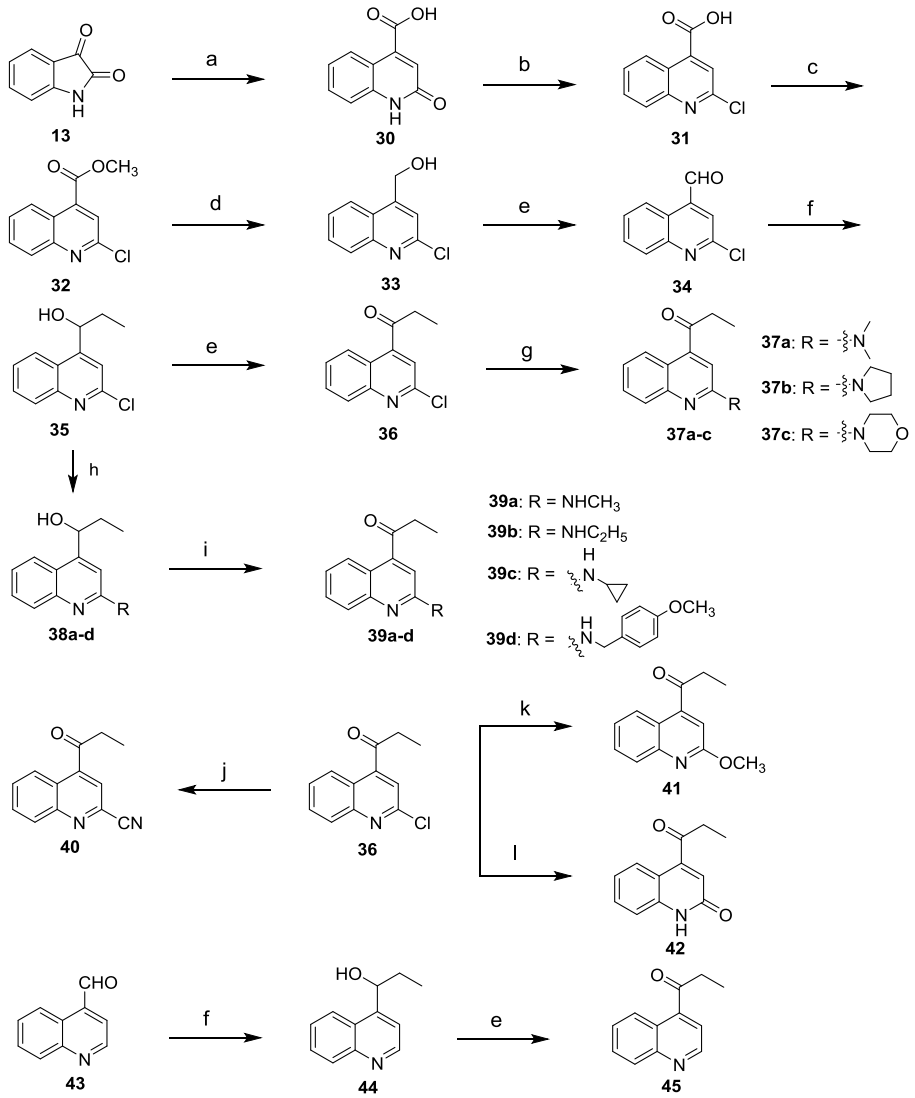

[a]Reagents and conditions: (a) malonic acid, AcOH, reflux, overnight, 85.6%; (b) $POCl_3$, reflux, 2 h, 72.3%; (c) i) oxalyl chloride, DMF (cat.), DCM, 0 ℃ - rt, 1 h; ii) C_2H_5OH, rt, 30 min, 72.0% over two steps; (d) $NaBH_4$, CH_3OH, 0 ℃ - rt, 2 h, 83.8%; (e) Dess-Martin reagent, DCM, 30 min, rt, moderate to high yields; (f) C_2H_5MgBr, THF, 0 ℃ - rt, 2 h, 72.9%; (g) various secondary amines, EtOH, 80 ℃, sealed tube, 81-88%; (h) various primary amines, EtOH, 150 ℃, sealed tube, 2 d, moderate yields; (i) IBX, DMSO, 30 min, rt, 45.0-56.9%; (j) $Pd(PPh_3)_4$, $Zn(CN)_2$, DMF, 120℃, 2 h, 87.0%; (k) $NaOCH_3$, CH_3OH, reflux, 4 h, 88.4%; (l) CH_3SO_2Na, H_2O, AcOH, 90 ℃, overnight, 87.3%.

The synthetic route of target compounds **29c-n** was outlined in Scheme 5. Intermediates **36**, **37a-c**, **39a-d**, **41**, **42** and **45** underwent aldol reactions with MEM protected isovanillin **25**, after which MEMs were removed to obtain target compounds **29c-m**. The cyano group hydrolyzed to ethyl ester led to compound **29n** in the aldo condensation reaction of intermediate **40** with **25**.

Scheme 5. The synthetic route of target compounds **29c-n**[a].

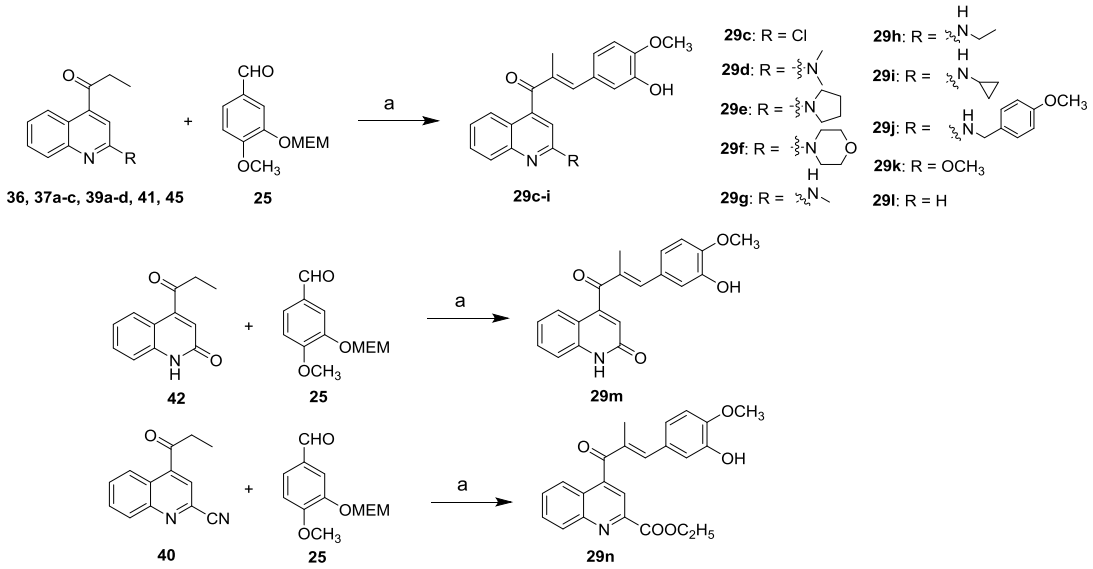

[a]Reagents and conditions: (a) i) NaOH, EtOH, rt, 30 min, moderate yields; ii) 10% HCl, EtOH, reflux, 30 min, 85-95%.

BIOLOGY

Antiproliferative Activities and the structure activity relationships (SARs). The *in vitro* antiproliferative efficacy of target compounds **24a-q** with a 2-methylquinoline moiety were first assessed by MTT assays using human chronic myelogenous leukemia cell K562 and compared to the reference compound CA-4. As shown in Table 1, except for compounds **24j-k** and **24n-o**, which had indole moieties

as ring B, all of the newly synthesized compounds exhibited decent antiproliferative activities in a nanomolar range. Among which, compounds **24b** and **24d**, featuring 3-amino-4-methoxyphenyl or 3-hydroxy-4-methoxyphenyl moieties, displayed the most potent activity with IC_{50} values of 0.011 and 0.009 μM, respectively, which were comparable to that of CA-4 (IC_{50} = 0.011 μM) and were approximately 6-fold more potent than the parent compound **1** (IC_{50} = 0.060 μM). The methyl substituent at the α-position of the unsaturated carbonyl group improved the activity (**24a** vs. **24b**, **24c** vs. **24d** and **24k** vs. **24l**), which was similar to the results in previous reports [21,22]. Additionally, different substituted indole derivatives **24i-q** were synthesized and evaluated for their antiproliferative activity. However, most of this series displayed lower activities (IC_{50} > 1 μM) than the phenyl counterparts, except compounds **24l** and **24m**, of which the unsaturated double bonds were substituted at the C-5 position on indole moiety. Besides, the methyl substituent at the *N*-1 position of the indole (**24m**) increased the activity for approximately 5-fold when compared to the non-substituted counterpart **24l**.

The effects of substitutions at the C-2 position on the quinoline moiety on activity were further investigated with both the isovanillic ring and methyl substituted α, β-unsaturated ketone retained. Thus, compounds **29a-n** with different substituted quinolines were synthesized and evaluated for their antiproliferative efficacy. As shown in Table 1, all compounds **29a-n** displayed decent activities except **29m**, which had a lactam rather than the quinoline ring. Steric hindrance of the groups at the C-2 position on the quinoline moiety seemed to exert a critical influence on the activity, as

compounds with smaller substitutions such as CH_3 (**24d**, IC_{50} = 0.009 μM), $NHCH_3$ (**29g**, IC_{50} = 0.018 μM), OCH_3 (**29k**, IC_{50} = 0.030 μM), and H (**29l**, IC_{50} = 0.015 μM) were more active than other compounds with larger groups. Interestingly, the CH_3 substituted compound **24d** exhibited a slightly more potent activity than the correspond non-substituted counterpart **29l**, though the methyl group has a larger steric hindrance than hydrogen.

The positive results of the antiproliferative activities of newly designed quinoline-chalcone derivatives against K562 cells led us to further evaluate the biological functions against more cancer cell lines. Four additional cancer cell lines, including human hepatocellular carcinoma (HepG2), epidermoid carcinoma of the nasopharynx (KB), human colon cancer cells (HCT-8) and human breast cancer cells (MDA-MB-231), were chosen for further evaluation. The cytotoxic data of representative compounds against these four cancer cell lines were shown in Table 2, which indicated that the IC_{50} values of selected compounds against these four cancer cell lines were in nanomolar ranges. The K562 cell was the most sensitive cell line among the five cancer cell lines tested, and the most active compound **24d** exhibited comparable activity to the reference compound CA-4 with IC_{50} values ranging from 0.009 to 0.016 μM. Notably, **24d** displayed an approximately 6-fold improvement in activity compared with the parent compound **1**. The SARs of the newly synthesized compounds were summarized in Figure 3.

Table 1. Antiproliferative activities of compounds **24a-q** and **29a-n** against K562 cell line[a].

Compd.	IC_{50} values (μM)[b]	Compd.	IC_{50} values (μM)[b]

	K562		K562
24a	0.850 ± 0.032	**29b**	0.110 ± 0.008
24b	0.011 ± 0.001	**29c**	0.053 ± 0.006
24c	0.127 ± 0.07	**29d**	0.049 ± 0.001
24d	**0.009 ± 0.001**	**29e**	0.315 ± 0.033
24e	0.108 ± 0.009	**29f**	0.153 ± 0.014
24f	1.055 ± 0.040	**29g**	0.018 ± 0.003
24g	0.069 ± 0.007	**29h**	0.040 ± 0.005
24h	0.563 ± 0.021	**29i**	0.058 ± 0.008
24i	> 1	**29j**	0.330 ± 0.028
24j	> 1	**29k**	0.026 ± 0.004
24k	> 1	**29l**	0.015 ± 0.001
24l	0.346 ± 0.015	**29m**	1.239 ± 0.055
24m	0.074 ± 0.009	**29n**	0.120 ± 0.015
24n	> 1	**1**	0.060 ± 0.007
24o	> 1	**CA-4**	0.011 ± 0.001
29a	0.050 ± 0.004		

[a] Cells were treated with different concentrations of the compounds for 72 h. Cell viability was measured by an MTT assay as described in the Experimental Section.

[b] IC_{50} values are indicated as the mean ± SD (standard deviation) of at least three independent experiments.

Table 2. Antiproliferative activities of representative compounds against four cancer cell lines[a].

Compd.	IC_{50} values (μM)[b]			
	HepG2	KB	HCT-8	MDA-MB-231
24a	0.223 ± 0.021	0.189 ± 0.015	0.21 ± 0.010	0.195 ± 0.011
24b	0.036 ± 0.008	0.025 ± 0.003	0.036 ± 0.005	0.063 ± 0.009
24c	0.121± 0.010	0.123 ± 0.022	0.137 ± 0.015	0.112 ± 0.013
24d	**0.015± 0.002**	**0.016 ± 0.001**	**0.015 ± 0.003**	**0.015 ± 0.004**
24l	0.226± 0.021	0.429 ± 0.034	0.421 ± 0.035	0.425 ± 0.025
24m	0.111± 0.009	0.124 ± 0.013	0.135 ± 0.011	0.220 ± 0.016
29a	0.165± 0.012	0.231 ± 0.022	0.242 ± 0.018	0.209 ± 0.015
29c	0.187± 0.014	0.237 ± 0.023	0.227 ± 0.026	0.183 ± 0.014
29d	0.057± 0.003	0.043 ± 0.008	0.052 ± 0.006	0.048 ± 0.005
29g	0.027± 0.003	0.029± 0.006	0.040 ± 0.009	0.043 ± 0.007
29k	0.038± 0.002	0.052 ± 0.006	0.061 ± 0.008	0.052 ± 0.008
29l	0.024± 0.001	0.026 ± 0.001	0.037 ± 0.003	0.030 ± 0.007
1	0.102± 0.010	0.108 ± 0.005	0.104 ± 0.010	0.102 ± 0.009
CA-4	0.012± 0.001	0.012 ± 0.002	0.015 ± 0.004	0.015 ± 0.003

[a] Cells were treated with different concentrations of the compounds for 72 h. Cell viability was measured by the MTT assay as described in the Experimental Section.

[b] IC_{50} values are indicated as the mean ± SD (standard deviation) of at least three independent experiments.

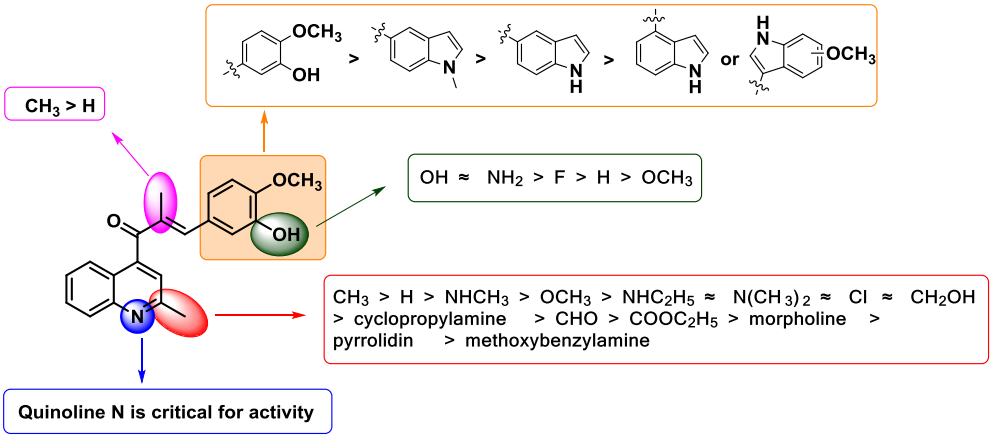

Figure 3. Summarized SARs of the new synthesized compounds.

Compound 24d Selectively Inhibited Cancer Cell Growth *In Vitro*. Nonselective cytotoxicity is one of the main factors limiting the clinical use of anticancer drugs.[41] To obtain insights into the cytotoxic potential of these new compounds on normal human cells, the effects of compounds **24b**, **24d**, **29g**, and **29l** were evaluated in the normal human liver cell line L-O2 with CA-4 as the reference, which were compared with the IC_{50} values against human hepatocellular carcinoma cells (HepG2). As shown in Table 3, all the tested compounds showed high selectivity in inhibiting the growth of HepG2 cells *vs.* L-O2 cells with selective index (SI) values (IC_{50} of normal cells/IC_{50} of tumor cells) ranging from 24.1 to 65.8 while the SI value of the reference CA-4 was only 7.9. Importantly, the most potent compound in cancer cell antiproliferative assays, **24d**, was the most selective with an SI value of 65.8. Thus, **24d** was chosen for further biological studies.

Table 3. Antiproliferative activities of compounds **24b**, **24d**, **29g**, **29k** and **29l** against normal human liver cell line L-02[a].

Compd.	IC_{50} values (μM)[b]		Selective Index[c]
	HepG2	L-O2	
24b	0.036 ± 0.008	0.923 ± 0.056	25.6
24d	0.015 ± 0.002	0.987 ± 0.064	**65.8**
29g	0.027 ± 0.003	1.086 ± 0.101	40.2
29k	0.038 ± 0.002	0.914 ± 0.091	24.1
29l	0.024 ± 0.001	0.928 ± 0.082	38.7
CA-4	0.012 ± 0.001	0.095 ± 0.012	7.9

[a] Cells were treated with different concentrations of the compounds for 72 h. Cell viability was measured by an MTT assay as described in the Experimental Section.

[b] IC_{50} values are indicated as the mean ± SD (standard deviation) of at least three independent experiments.

[c] Selectivity index = (IC_{50} L-O2)/(IC_{50} HepG2).

Compound 24d Inhibited Tubulin Polymerization and Colchicine Binding Effects. To investigate whether the antiproliferative activity of compound **24d** was related to interactions with microtubule systems, **24d** was evaluated for *in vitro* microtubule polymerization activity. The typical microtubule depolymerization agent (MDA) colchicine was employed as the reference. As shown in Figure 4, compound **24d** displayed a concentration-dependent inhibition of tubulin polymerization, indicating that the mechanism of **24d** was consistent with colchicine as an MDA. Moreover, **24d** exhibited more potent tubulin polymerization inhibitory activity (IC_{50} = 1.71 μM) than CA-4 (IC_{50} = 2.53 μM) (Table 4). In addition, **24d** competed with

[3H]-colchicine in binding to tubulin. The binding potency of **24d** to the colchicine binding site was comparable to that of CA-4 with the inhibition rates of 79.4% and 92.7% at 1 μM and 5 μM, respectively (Table 4), indicating that **24d** bound to the colchicine binding site similar to CA-4.

Compound 24d Disrupted the Organization of the Cellular Microtubule Network in K562 cells. The inhibitory effects of **24d** on microtubule organization were further investigated by immunofluorescent staining in K562 cells. As shown in Figure 5, the microtubule networks in vehicle-treated cells had a normal arrangement with slim and fibrous microtubules wrapped around the cell nucleus. However, after exposure to **24d** at three different concentrations (5 nM, 10 nM, and 20 nM) for 24 h, the microtubule organization in the cytosol were disrupted especially for the group that was treated with **24d** at 30 nM, indicating that **24d** induced disruption of the microtubule networks, which might eventually lead to cell apoptosis.

Table 4. Inhibition of Tubulin Polymerization[a] and Colchicine Binding to Tubulin[b].

Compd.	Inhibition of tubulin polymerizaion	Inhibition of colchicine binding (%) inhibition ± SD	
	IC_{50} (μM)	1 μM	5 μM
24d	1.71 ± 0.08	79.4 ± 4.4	92.7 ± 4.7
CA-4	2.53 ± 0.19	81.2 ± 1.9	93.7 ± 4.4

[a] The tubulin assembly assay measured the extent of assembly of 2 mg/mL tubulin after 60 min at 37 °C. Data are presented as the mean ± SD from three independent experiments.

[b] Tubulin, 1 μM; [3H]-colchicine, 5 μM; and inhibitors, 1 or 5 μM.

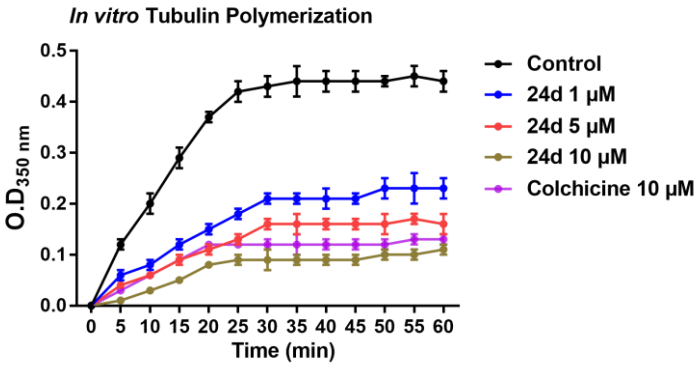

Figure 4. Effect of **24d** on tubulin polymerization *in vitro*. Purified tubulin protein at 2 mg/mL in a reaction buffer incubated at 37 °C in the presence of 1% DMSO, test compounds (**24d** at 1, 5, or 10 μM) or colchicine (10 μM). Polymerizations were followed by an increase in fluorescence emission at 350 nm over a 60 min period at 37 °C. The experiments were performed three times.

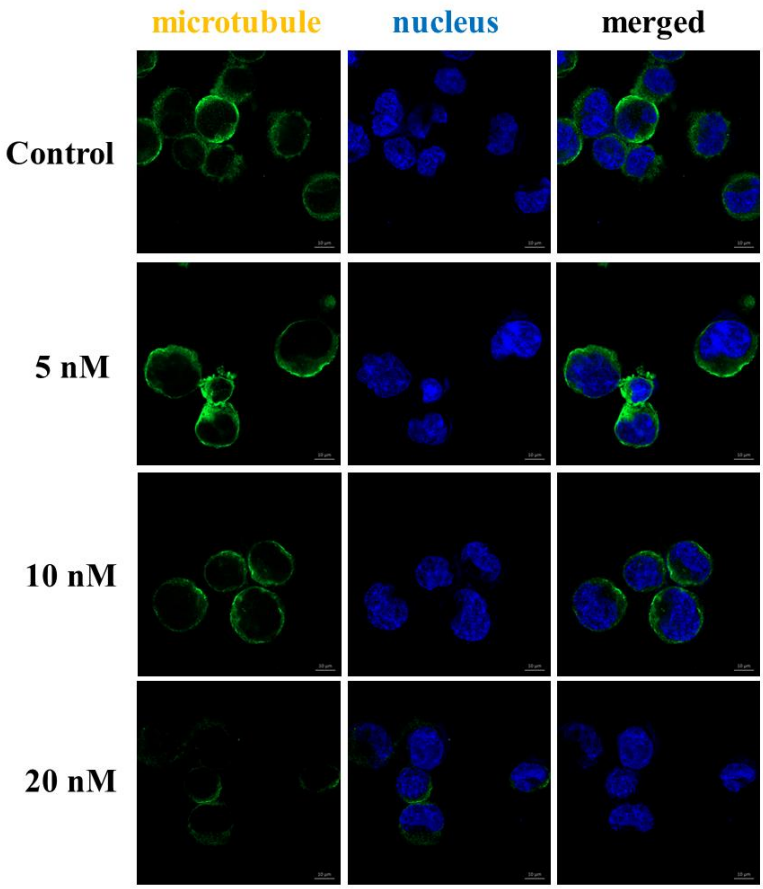

Figure 5. Effects of **24d** on the cellular microtubule network visualized by immunofluorescence.

K562 cells were treated with vehicle control 0.1% DMSO, **24d** (5 nM, 10 nM, and 20 nM). Then, the cells were fixed and stained with anti-α-tubulin-FITC antibody (green), Alexa Fluor 488 dye and counterstained with DAPI (blue). The detection of the fixed and stained cells was performed with an LSM 570 laser confocal microscope (Carl Zeiss, Germany).

Docking Studies of Compound 24d with Tubulin. To investigate the potential binding site of **24d** with the tubulin-microtubule system, molecular modeling studies were performed. The crystal structure of tubulin complexed with CA-4 (PDB: 5lyj) [42] was chosen as the docking protein. CA-4 was first redocked into the colchicine site with the resulting root mean square deviation (RMSD) value of 0.69 Å, which indicated our docking method was reasonable. As shown in Figure 6a, **24d** adopted a very similar location with that of CA-4. The phenolic hydroxyl of **24d** formed two hydrogen bonds with the residue Val 315 while the hydroxyl of CA-4 interacted with the residue Thr 179. The *N*-1 atom on the quinoline moiety of **24d** formed a hydrogen bond with the critical residue Cys 241, which was similar to the binding pose of compound **11** with tubulin.[33] The C-2 methyl group of **24d** pointed towards the deep pocket of the colchicine site, which might explain how the C-2 position tolerated a modification without a significant decrease in activity. Similarly, the parent compound **1** was also docked into the colchicine site, and the result showed that compound **1** and **24d** adopted similar positions when binding to tubulin (Figure 6b). The docking results demonstrated that **24d** binds to the colchicine site of tubulin resembling the binding mode of CA-4.

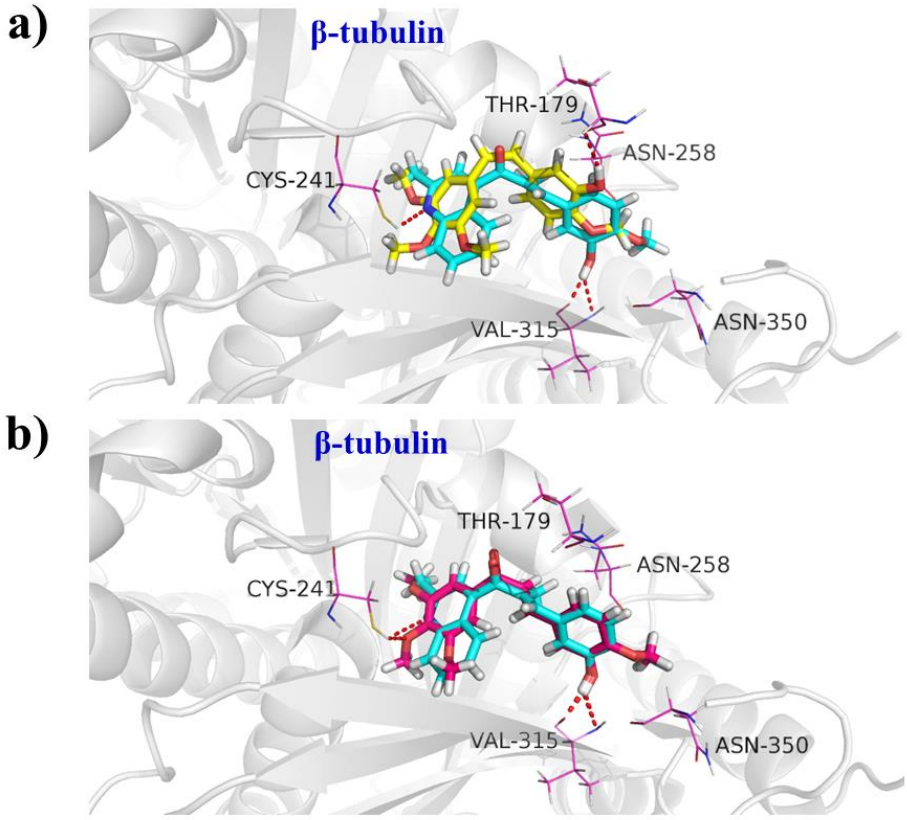

Figure 6. Proposed binding models for **24d** binding with tubulin (PDB code: 5lyj). (a) CA-4 (shown in yellow) and **24d** (shown in cyan); (b) **1** (shown in pink) and **24d** (shown in cyan).

Compound 24d Induced G2/M Phase Arrest via Regulating G2/M-Related Protein Expression. Since most tubulin polymerization inhibitors could disrupt the regulated cell cycle distribution,[43] a flow cytometry analysis was performed to examine the arrest effects of **24d** on cell cycle of K562 cells. As illustrated in Figure 7a and 7c, incubation with **24d** arrested the cell cycle at the G2/M phase. The incubation of K562 cells with increasing concentrations of **24d** from 0 to 30 nM increased the percentage of cells in the G2/M phase from 15.82% to 26.98%.

Mitosis in eukaryotic cells is regulated by the activation of Cdc2 kinase, which is controlled by several steps including cyclin B1 binding and cdc25c phosphorylation.[44]

Thus, to obtain insight into the mechanism of **24d** in K562 cell cycle arrest, the expression of cell cycle regulatory proteins was investigated. As shown in Figure 7b and 7d, **24d** decreased cdc2, cyclin B1 and cdc25c protein levels in a concentration-dependent manner. The results suggested that the **24d**-induced G2/M arrest may be correlated with a change of expression of cdc2/cyclin B1 and cdc25c.

Compound 24d Induced Apoptosis via Regulating of Apoptosis-related Protein Expressions. Mitotic arrest of tumor cells by microtubule targeting agents is generally associated with cellular apoptosis.[45] Hoechst 33342 staining was first used to assess morphology changes of K562 cells, as shown in Figure 8a, K562 cells incubated with **24d** (5, 10, and 20 nM) for 48 h displayed significant changes in cell morphology, such as nucleus fragmentation and chromatin condensation, indicating cell apoptosis. To further evaluate the capacity of **24d** to induce apoptosis, Annexin-V/PI assay was performed with K562 cells. As shown in Figure 8b and 8d, after K562 cells were exposed to 5, 10, and 20 nM of **24d** for 48 h, the total numbers of early (Annexin-V+/PI−) and late (Annexin-V+/PI+) apoptotic cells were 17.21%, 34.55% and 60.14%, respectively.

Increasing evidence has indicated that the regulation of the Bcl-2 family of proteins is involved in the signaling pathways,[46] including pro-apoptotic (e.g., Bax and Bad) and anti-apoptotic proteins (e.g., Bcl-2 and Bcl-xl). As shown in Figure 8c and 8e, **24d** upregulated Bad and Bax and downregulated Bcl-2 and Bcl-xl protein levels in a concentration-dependent manner. Thus, as described above, compound **24d** induced cell apoptosis by interfering with the expression of apoptosis-related proteins.

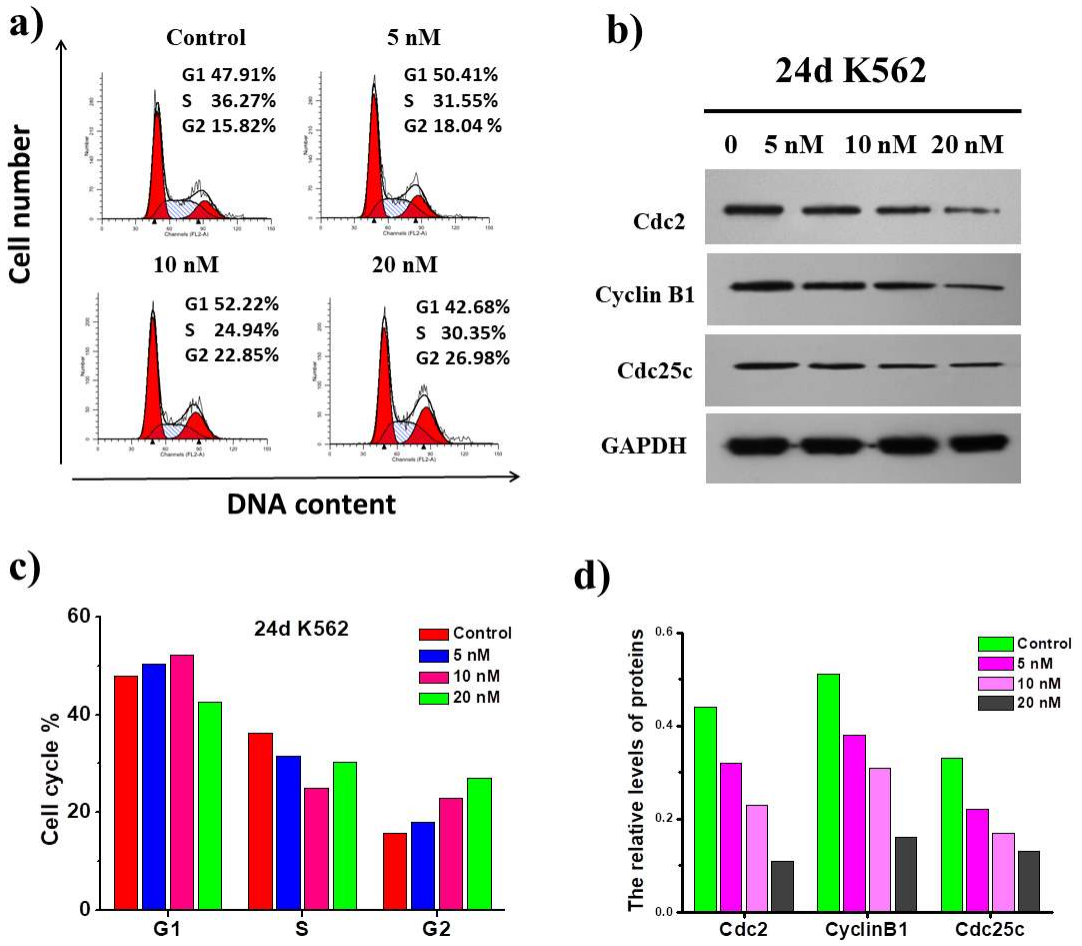

Figure 7. Compound **24d** induced G2/M arrest in K562 cancer cells. (a) K562 cells were incubated with DMSO and varying concentrations of **24d** (5, 10, and 20 nM) for 48 h. Cells were harvested and stained with PI and then analyzed by flow cytometry. The percentages of cells in different phases of the cell cycle were analyzed by ModFit 4.1. (b) Western blotting analysis on the effect of **24d** on the G2/M regulatory proteins. The cells were harvested and lysed for the detection of cdc2, cdc25c and cyclin B1. (c) Histograms display the percentage of cell cycle distribution. (d) Histograms display the density ratios of cdc2, cdc25c and cyclin B1 to GADPH.

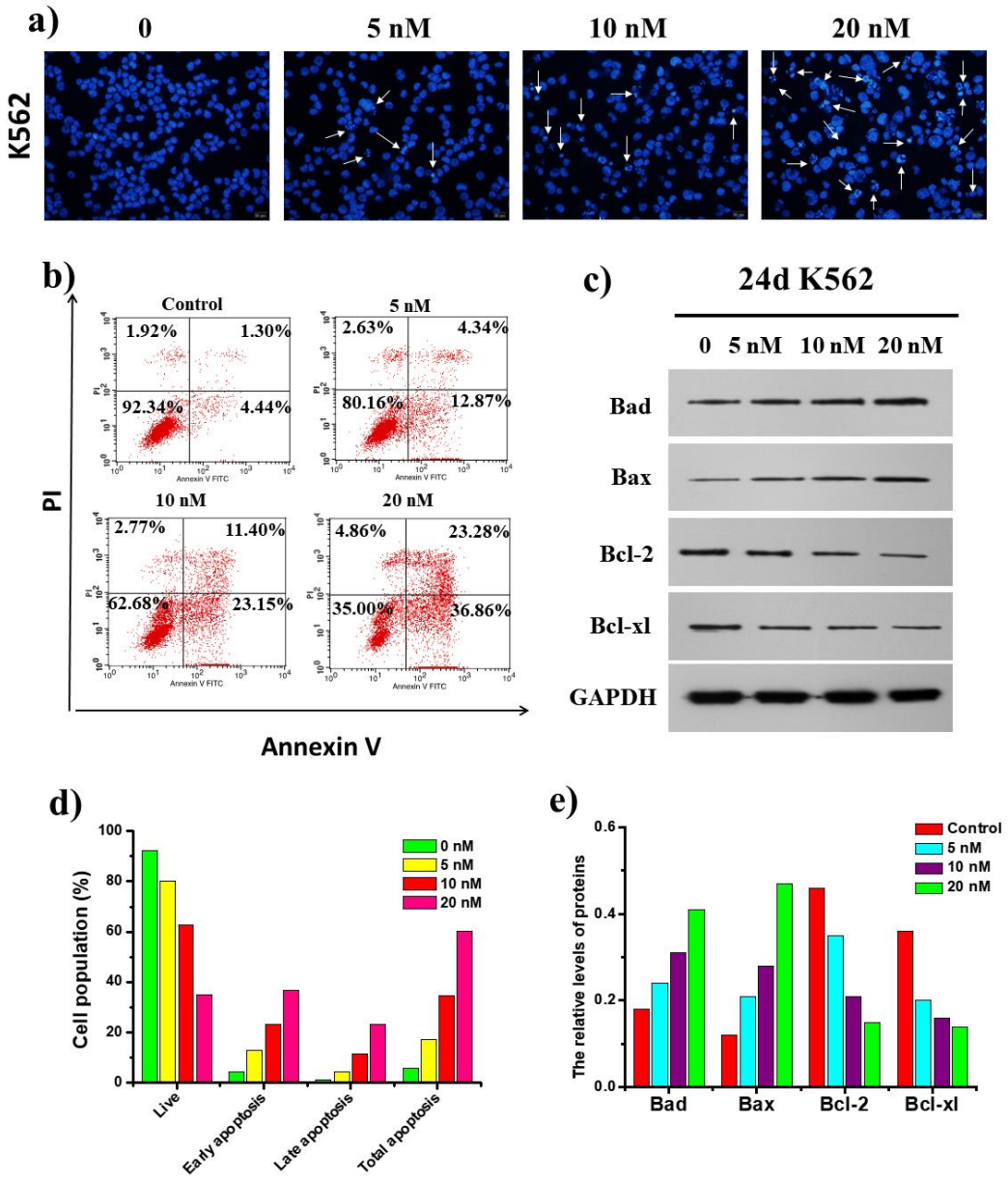

Figure 8. Compound **24d** induced apoptosis in K562 cancer cells. (a) Cell morphological alterations and nuclear changes (white arrow marked cells) associated with K562 cells after incubation with **24d** (5, 10, and 20 nM) for 48 h were assessed by staining with Hoechst 33342 and visualized by fluorescence microscopy; (b) K562 cells were incubated with DMSO and varying concentrations of **24d** (5, 10, and 20 nM) for 48 h, cells were collected and stained with Annexin V/PI, followed by flow cytometric analysis; (c) Western blotting analysis on the effect of **24d** on apoptosis-related proteins. The cells were harvested and lysed to detect Bad, Bax, Bcl-2

and Bcl-xl; (d) Histograms display the percentage of cell distribution; (e) Histograms display the density ratios of Bad, Bax, Bcl-2 and Bcl-xl to GADPH.

Compound 24d Induced Mitochondrial Depolarization and Reactive Oxygen Species (ROS) Generation. Increasing evidence has indicated that mitochondria plays an important role in regulating cellular functions, and mitochondrial dysfunction is involved in many pathological processes.[47] To explore whether **24d** could induce mitochondrial dysfunction, mitochondrial membrane potential (MMP) assay by JC-1 staining of mitochondria in K562 was performed. As shown in Figure 9a, with the concentrations of **24d** increasing from 0 to 20 nM, the green fluorescence intensity (JC-1 monomers, low mitochondrial membrane potentials) correspondingly increased from 0.63% to 53.39%, suggesting that **24d** caused MMP collapse of K562 cells and mitochondrial dysfunction, which eventually triggers apoptotic cell death.

Accumulating evidence reveals that increased levels of reactive oxygen species (ROS) is often associated with promoting cancer cell growth,[47] and mitochondrial membrane depolarization is related to mitochondrial production of ROS.[48] Thus, the fluorescent probe 2′,7′-dichlorofluorescein diacetate (DCF-DA) was used to evaluate the intracellular ROS levels after incubation with **24d**. As shown in Figure 9b and 9c, **24d** induced intracellular ROS generation with a dose-dependent manner, while the increased ROS was inhibited by pre-incubation with 2.5 mM of the ROS scavenger, *N*-acetyl cysteine (NAC).

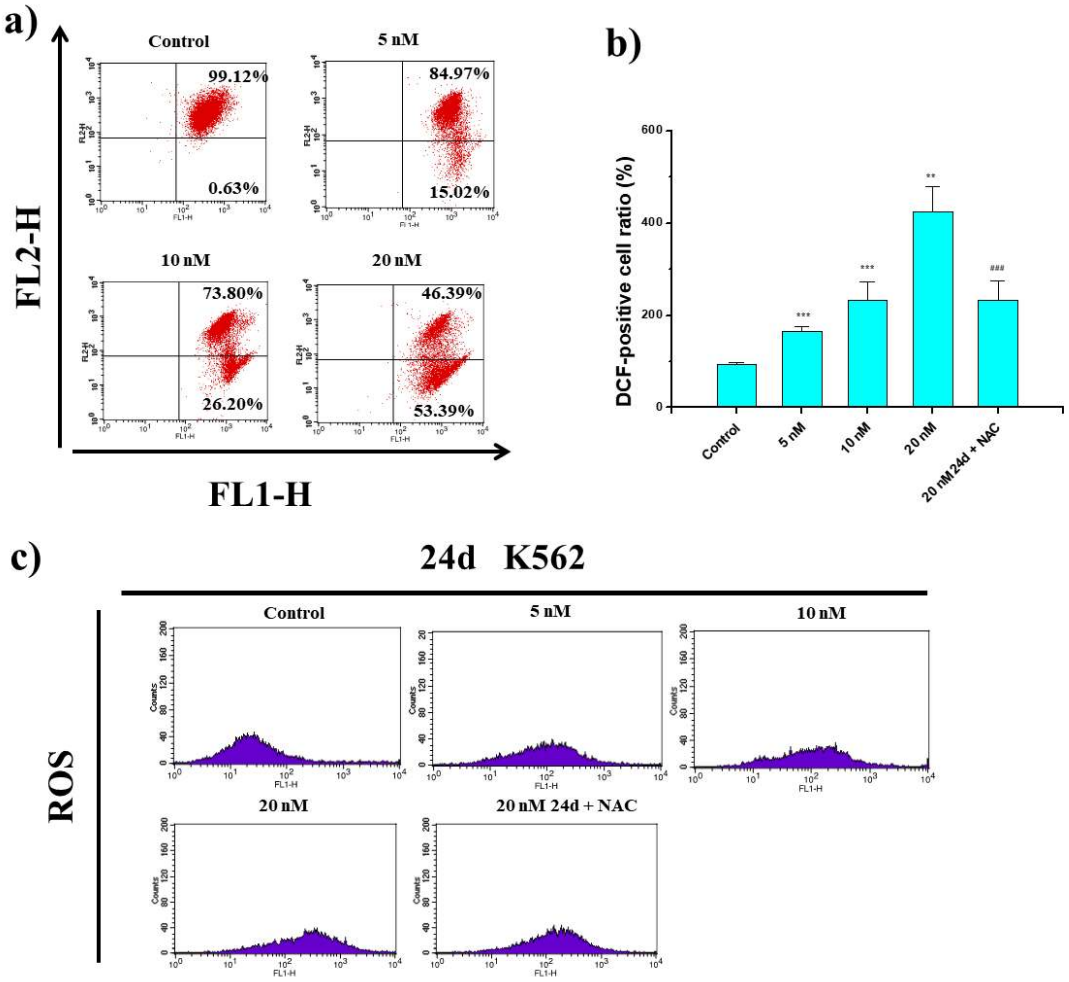

Figure 9. Effects of **24d** on the mitochondrial membrane potential of K562 cells. a) After incubation with different concentrations (0, 5, 10 and 20 nM) of **24d** in K562 cells for 48 h prior to staining with JC-1 dye, the number of cells with collapsed mitochondrial membrane potentials was determined by flow cytometry analysis; (b) Histograms display the intracellular ROS contents in the absence or presence of **24d**. $^{**}p < 0.01$, $^{***}p < 0.001$ *vs.* control; ### $p < 0.001$ *vs.* 20 nM **24d**-treated group; (c) The generation of ROS was measured using the ROS-detecting fluorescent dye DCF-DA in combination with FACScan flow cytometry.

Compound 24d Inhibited the Migration and Invasion of MDA-MB-231 Cells. Cell migration and invasion play essential roles in achieving normal functions, such as wound healing and embryonic growth.[49] Drugs that can simultaneously induce

apoptosis and inhibit migration or invasion of cancer cells have clinical superiorities and have gained increasing research interest.[50] To evaluate the ability of **24d** in preventing the migration and invasion of cancer cells, transwell assays with or without Matrigel were conducted. The highly invasive and aggressive MDA-MB-231 cell line was chosen for activity evaluation. As shown in Figure 10a and 10b, **24d** dose-dependently inhibited MDA-MB-231 cell migration through the membrane of the transwell insert after incubation with **24d** (2, 5, and 10 nM) for 48 h. In the invasion assay, **24d** potently and dose-dependently inhibited cell invasion through the Matrigel-coated membrane (Figure 10c and 10d). These results indicated that **24d** effectively inhibited the migration and invasion of MDA-MB-231 cells, which were not due to the cytotoxic actions of **24d** (inhibitive rate under 10% after incubation with **24d** at 10 nM for 48 h).

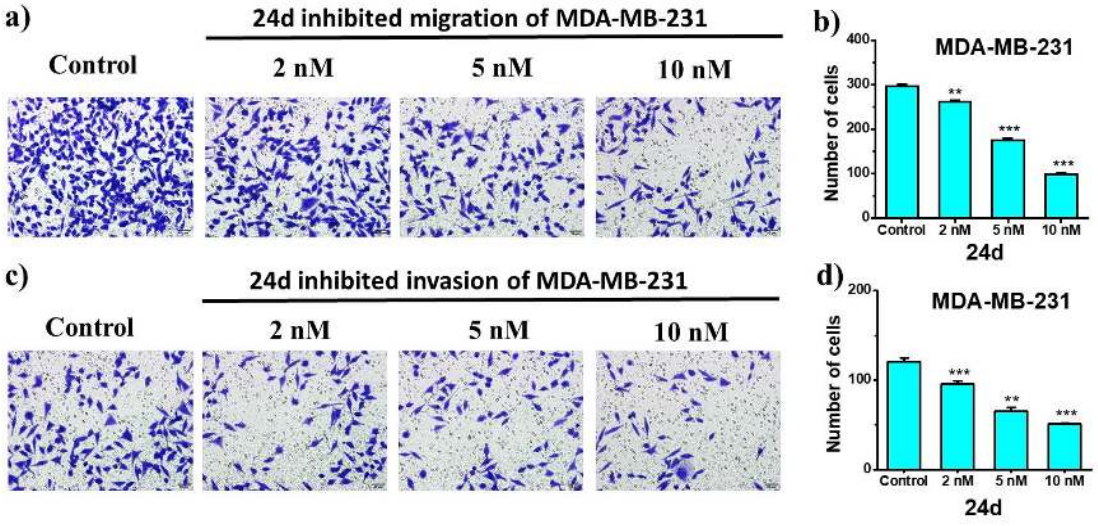

Figure 10. Effects of **24d** on transwell migration and invasion of MDA-MB-231 cells. (a) The MDA-MB-231 cells were seeded on chambers and incubated with **24d** (0, 2, 5, and 10 nM) for 48 h. Cells that migrated through the chambers were stained with crystal violet, and representative

images were captured; (b) The cells that migrated through the chambers were counted from three independent experiments; (c) The MDA-MB-231 cells were seeded on chambers and and incubated with **24d** (2, 5, and 10 nM) for 48 h. Cells that migrated through the Matrigel-coated chambers were stained with crystal violet, and representative images were captured; (d) The cells that migrated through the Matrigel-coated chambers were counted from three independent experiments. All the data in (b and d) were expressed as the means ± SD of each group of cells. $^{**}P < 0.01$, $^{***}P < 0.001$ *vs*. control group.

Compound 24d Exhibited Potent Anti-Vascular Activity. Most microtubule binding agents possess potent vascular disrupting activity, which are contributed to the disruption of microtubule dynamics to induce endothelial cell shape change.[51] As HUVEC migration is the key step to generate new blood vessels, [52] wound healing assay was applied to assess the ability of **24d** to inhibit HUVEC migration. As shown in Figure 11a and 11c, the untreated cells migrated to fill the area that was initially scraped after 24 h, while **24d** significantly inhibited HUVEC migration at the dose of 20 nM.

We also evaluated the effect of **24d** in a tube formation assay, which are based on the ability of HUVECs to form tubular and cord-like networks on Matrigel. In contrast to the tube-like networks of the control, the capillary-like tubes of HUVECs exposed to **24d** at doses of 5, 10, and 20 nM for 6 h could be interrupted at different levels (Figure 11b). These results showed that **24d** effectively inhibited the tube formation of HUVECs.

The antiproliferative activity of **24d** against HUVECs was also determined by an

MTT assay to exclude the possibility that the anti-vascular activity of **24d** was due to a cytotoxic action of **24d**. The calculated IC_{50} value of **24d** against HUVECs after a 24-h treatment was 0.250 ± 0.06 μM, which is higher than the concentration of 10 nM required for the obvious inhibition of cell migration and tube formation. These results indicate that **24d** exhibited possessed anti-vascular activity.

Physicochemical Properties of 24d. To evaluate the drug-likeness of **24d**, the physicochemical properties of **24d** were predicted with compound **1** and CA-4 as the references.[53] As shown in Table 5, compound **24d** conformed to Lipinski's rule of five. The aqueous solubility in phosphate buffer (pH 7.4) was also determined at 20 °C by HPLC.[54] As shown in Table 5, the solubility of **24d** was approximately 5- and 16-fold greater than compounds **1** and CA-4, respectively. Moreover, the hydrochloride salt of **24d** (**24d-HCl)** could be easily prepared by the reaction of **24d** with hydrogen chloride in ethyl acetate, which was soluble in PBS (solubility > 1000 μg/mL). The improvement of the aqueous solubility of **24d** is most likely attributable to the quinoline moiety, which is more water-soluble than trimethylphenyl ring in compounds **1** and CA-4.

Table 5. Aqueous Solubility in PBS (pH 7.4) and Physicochemical Properties of Compounds **1**, CA-4, and **24d**.

Compd.	MW[a]	HBA[b]	HBD[c]	cLogP[d]	tPSA[e]	Solubility (μg/mL)[f]
1	344.13	6	1	2.78	74.23	3.2
CA-4	316.13	5	1	3.47	57.16	1.0 [55]
24d	333.14	4	1	4.37	59.42	16.0

24d-HCl	-	-	-	-	-	> 1000
RO5[g]	< 450	< 10	< 5	< 5	< 90	

[a]MW: molecular weight; [b]HBA: hydrogen-bond acceptor atoms; [c]HBD: hydrogen-bond donor atoms; [d]clogP: calculated logarithm of the octanol-water partition coefficient; [e]tPSA: topological polar surface area, calculated using http://www.molinspiration.com/cgi-bin/properties. [f]Solubility in PBS (pH 7.4); [g]RO5: Lipinski's rule of five.

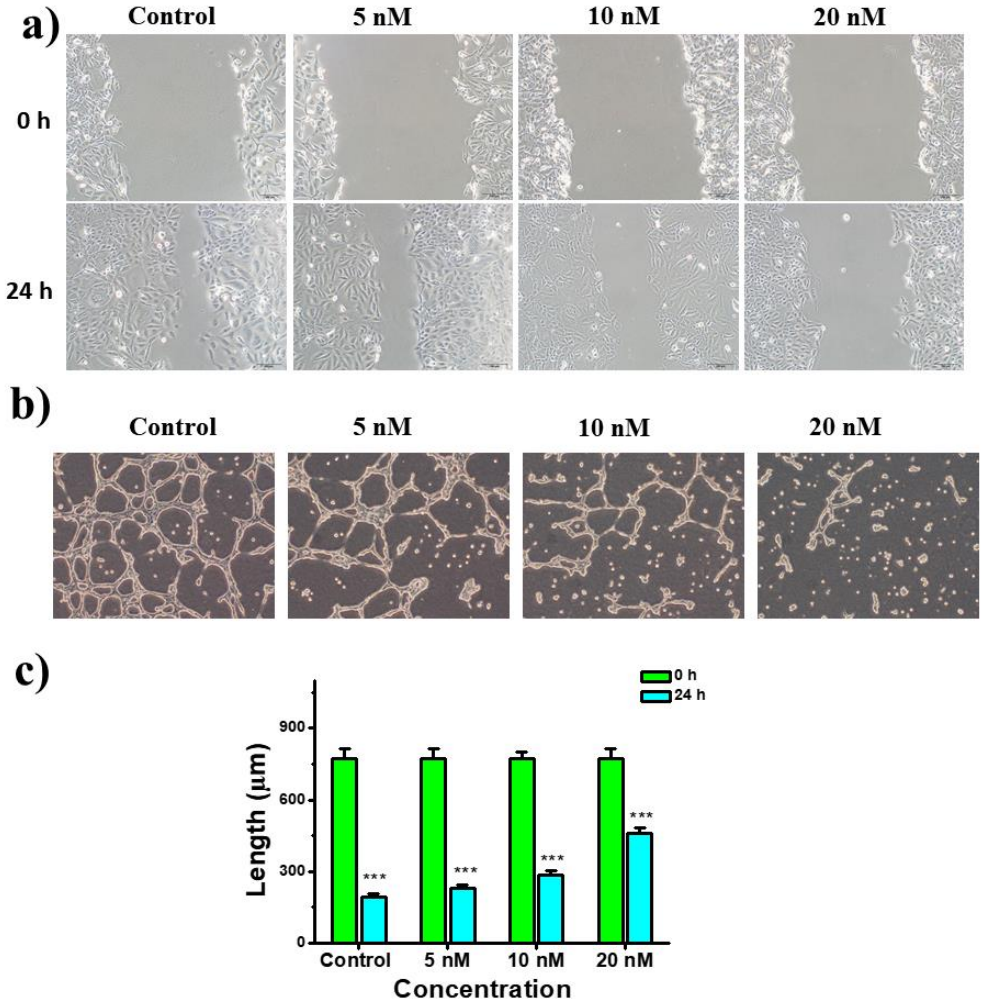

Figure 11. Effects on HUVECs migration and tube formation. (a) Scratches were created with sterile 200 μL pipette tips, and images were captured using phase contrast microscopy at 0 h and 24 h after treatments with 0, 5, 10 and 20 nM of **24d**. (b) Images depicting the formation of a HUVEC capillary-like tubular network after treatments with 0, 5, 10 and 20 nM of **24d** for 6 h. (c)

Histograms display the length of the scratches at 0 h and 24 h after treatments with 0, 5, 10 and 20 nM of **24d**, ***$P < 0.001$ *vs*. control group.

The Safety Profile of 24d in Mice. To investigate the safety profiles of **24d**, the acute toxicity was determined in ICR mice treated with 409.6, 512, 640, 800, and 1000 mg/kg (*iv*, n = 10 per group) for 14 days. As shown in Table 6, treatment with **24d** at doses of 409.6 mg/kg only caused one death in ten mice, while treatment with **24d** at 1000 mg/kg killed nine mice. Finally, the median lethal dose (LD_{50}) value of **24d** was calculated to be 665.62 mg/kg, indicating the low toxicity of **24d** and its safety as an anti-tumor agent.

Table 6. Acute Toxicity of **24d** in Mice.

dose (mg/kg)	no. of mice	total mortality	survival (%)	LD_{50} (mg/kg)[a]
409.6	10	1	90	
512	10	2	80	
640	10	4	60	665.62
800	10	7	30	
1000	10	9	10	

[a]The 95% confidence limits: 624.01−710.02 mg/kg.

24d and 24d-HCl Inhibited the Growth of H22 Xenograft Tumors in Mice. The *in vivo* anti-tumor efficacy of **24d** and **24d-HCl** were further evaluated in mouse liver cancer xenograft models, which were established by subcutaneous inoculation of H22 cells into the right flank of mice. Once the tumors were well-established, the mice

were randomly allocated into eight groups: vehicle (*iv*, group 1), paclitaxel (PTX) (*iv*, 8 mg/kg per 2 days, group 2), **24d** (*iv*, 10 mg/kg per day, group 3), **24d** (*iv*, 20 mg/kg per day, group 4), **24d-HCl** (*iv*, 10 mg/kg per day, group 5), **24d-HCl** (*iv*, 20 mg/kg per day, group 6), CA-4 (*iv*, 10 mg/kg per day, group 7), and CA-4 (*iv*, 20 mg/kg per day, group 8), with eight mice per group (Figure 12a). As shown in Figure 12b and 12d, **24d** and **24d-HCl** significantly and dose-dependently decreased tumor volume and tumor weight. At the 20 mg/kg dose, **24d-HCl** reduced the tumor weight by 68.9%, which was more potent than the free drug **24d** (65.3%). Although CA-4 displayed comparable *in vitro* antiproliferative activity to **24d**, its anti-tumor activity (inhibition rate: 55.3% at 20 mg/kg) was less potent than **24d.** Additionally, PTX exhibited potent activity with an inhibition rate of 90.4% at a dose of 8 mg/kg every 2 days. However, PTX-treated mice displayed significant decrease of body weight compared to those in control group (Figure 12c) while **24d** and **24d-HCl** did not obviously affect the body weight at doses of 10 and 20 mg/kg.

Furthermore, we also observed the impact of **24d** on tumor microvessels *in vivo* by immunohistochemistry. Tumor vessels were stained with CD31, which is a prominent endothelial marker that binds specifically to blood microvessels. As shown in Figure 12e, **24d**-treated group at the dose of 20 mg/kg displayed considerably lower tumor microvessel density (MVD) than the control group, indicating that **24d** exhibited potent *in vivo* anti-vascular activity.

Additionally, H&E staining of the heart, liver, spleen, lung and kidney collected at the end of the study also suggested no observable major organ-related toxicities

(Figure 13). Overall, these data indicated that compound **24d** was efficacious in inhibiting the growth of cancer *in vivo* with no observable toxicity. It deserves further evaluation as a safe anti-tumor agent.

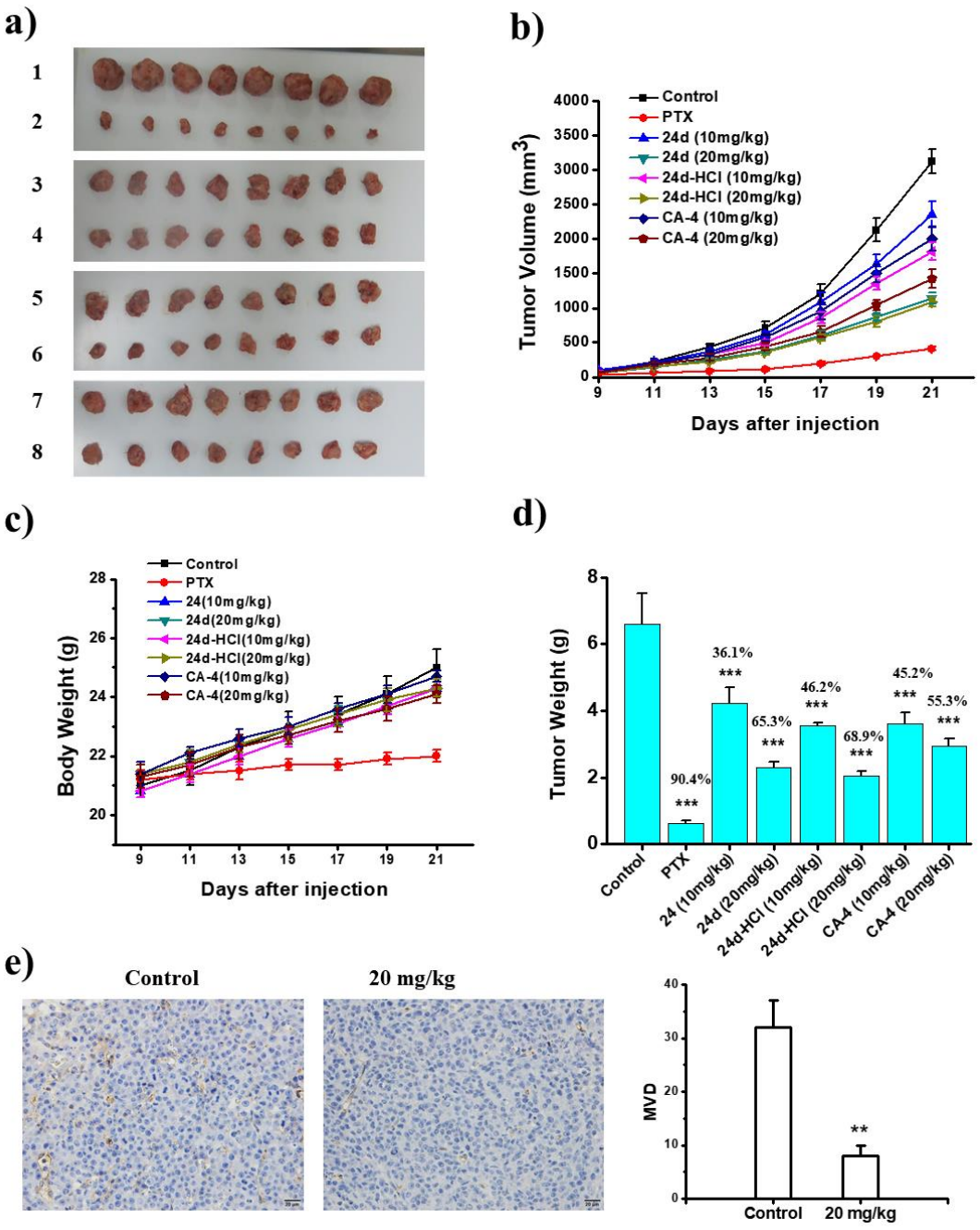

Figure 12. **24d** inhibits liver cancer xenograft growth *in vivo*. After administering vehicle (group 1), PTX (8 mg/kg per 2 days, group 2), **24d** (10 mg/kg per day, group 3), **24d** (20 mg/kg per day, group 4), **24d-HCl** (10 mg/kg per day, group 5), **24d-HCl** (20 mg/kg per day, group 6), CA-4 (10

mg/kg per day, group 7), and CA-4 (20 mg/kg per day, group 8) for three weeks, the mice were sacrificed, and the tumors were weighed. (a) The images of tumors from mice at 21 days after initiation of treatment. (b) Tumor volume changes during treatment. (c) Body weight changes of mice during treatment. (d) The weight of the excised tumors of each group. ***$P < 0.001$ *vs*. control group. (e) Immunohistochemical staining against CD31 was used to quantify the microvessel density (MVD) in H22 xenograft tumors treated with vehicle and **24d** (20 mg/kg). Representative images of anti-CD31 immunohistochemistry from five tumor xenografts are shown. **$P < 0.01$ *vs*. control group.

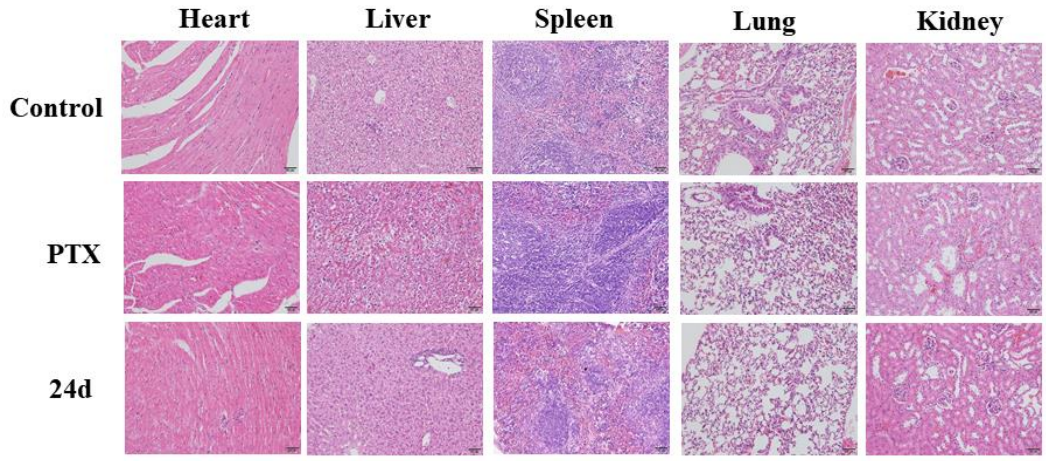

Figure 13. HE staining of heart, liver, spleen, lung and kidney of mice. No abnormality of these organs was observed.

CONCLUSION

Based on the previous work, we have continued to focus our studies on the new nitrogenous chalcones acting as CBSIs. With chalcone compound **1** as the parent compound, we designed and synthesized a series of novel quinoline-chalcone derivatives with comprehensive and detailed SARs. Some compounds displayed enhanced antiproliferative efficacy in a panel of human cancer cell lines, and the most

potent compound **24d** exhibited excellent antiproliferative activity with IC_{50} values ranging from 0.009 to 0.016 μM, which is comparable to those of the reference compound CA-4. Furthermore, **24d** displayed a 65.8-fold selectivity ratio for normal human liver L-O2 cells, which was higher than that of CA-4, indicating that **24d** might have lower toxicity than CA-4.

In addition, the microtubule polymerization inhibitory action of **24d** was investigated using an *in vitro* tubulin polymerization assay, colchicine competition inhibition assay, immunofluorescence analysis of intracellular microtubules and a virtual molecular docking study. These experiments demonstrated that **24d** effectively inhibited tubulin polymerization, and it bound to the colchicine site of tubulin. Further mechanistic studies indicated that **24d** induced cell cycle arrest in the G2/M phase via regulation of G2/M-related protein expression (cdc2, cyclin B1, and cdc25c) and induced cell apoptosis by upregulating the expression of pro-apoptotic protein (Bad and Bax) and downregulating the expression of anti-apoptotic protein (Bcl-2 and Bcl-xl). Additionally, **24d** depolarized the mitochondria membrane potentials and induced ROS generation in K562 cells.

Furthermore, **24d** inhibited the migration and invasion of MDA-MB-231 cells in transwell migration and invasion assays, indicating the potent anti-metastatic activity of **24d**. The anti-vascular activity of **24d** was confirmed in *in vitro* HUVECs migration and tube formation assays, and *in vivo* microvessel formation in H22 xenograft tumor issues. In addition, **24d** displayed satisfactory physicochemical properties conforming to Lipinski's rule of five, and its aqueous solubility was greatly

improved compared with compound **1** and CA-4. More importantly, **24d** have a safety profile with an LD_{50} value of 665.62 mg/kg after *iv.* injection, and **24d** and **24d-HCl** exhibited potent anti-tumor activities in mouse liver cancer xenograft models without observable major organ-related toxicities. **24d** effectively suppressed the tumor volume and reduced tumor weight by 65.3% at 20 mg/kg per day (*iv*). In the meantime, the more water-soluble hydrochloride salt **24d-HCl** displayed a higher inhibition rate of 68.9% at 20 mg/kg per day (*iv*), which is more potent than the reference CA-4.

Collectively, the new developed quinoline-chalcone derivative **24d** has been shown to possess significant *in vitro* anti-metastatic activity, anti-vascular and anti-tumor activities both *in vitro* and *in vivo*. Thus, **24d** has the potential to be further developed as an efficient chemotherapeutic agent.

EXPERIMENTAL SECTION

1. Chemistry.

1.1 General Methods. All commercially available reagents were used without further purification. Solvents were dried through routine protocols. Flash column chromatography was carried out on 200-300 mesh silica gel (Qingdao Haiyang Chemical, China). Reactions were monitored by thin-layer chromatography (TLC) on 0.25 mm silicagel plates (GF254) and visualized under UV light. ^{1}H NMR and ^{13}C NMR spectra were recorded with a Bruker AV-300 spectrometer (Bruker Company, Germany) in the indicated solvents ($CDCl_3$ or DMSO-d_6, TMS as internal standard):

the values of the chemical shifts are expressed in δ values (ppm) and the coupling constants (J) in Hz. Low- and high-resolution mass spectra (LRMS and HRMS) were measured on Finnigan MAT 95 spectrometer (Finnigan, Germany). Purity of all tested compounds was ≥ 95%, as estimated by HPLC (SHIMADZU Labsolutions, UV dection at λ = 254 nm) analysis on the Aglilent C18 column (4.6 × 150 mm, 5 μm).

1.2 1-(2-Methylquinolin-4-yl)ethan-1-one (16). 2-Methylquinoline-4-carboxylic acid (**14**) was synthesized according to literature report.[56] To a solution of **14** (500 mg, 2.7 mmol) in 20 mL anhydrous CH_2Cl_2 was added dimethylamine hydrochloride (310 mg, 3.2 mmol), trimethylamine (440 μL, 3.2 mmol), EDCI (1.0 g, 5.4 mmol), HOBt (437.4 mg, 3.2 mmol) and catalytic amount of DMAP. The mixture was stirred for 2 h, and extracted with CH_2Cl_2 (3 × 50 mL). The combined organic layers were then washed with brine, dried over anhydrous Na_2SO_4, and concentrated in vacuo to afford **15** as a yellow solid (510 mg, yield 83.1%), which was used for next step without further purification. A solution of CH_3MgBr in diethyl ether (3 M, 2.0 mL, 5.9 mmol) was added dropwise to a solution of **15** (500 mg, 2.7 mmol) in 20 mL anhydrous THF under nitrogen atmosphere at 0 °C. After stirring for 2 h, the reaction was quenched by NH_4Cl aqueous, and extracted with CH_2Cl_2 (3 × 50 mL). The combined organic layers were then washed with brine, dried over anhydrous Na_2SO_4, and concentrated in vacuo to provide the crude product, which was purified by column chromatography with petroleum/ethyl acetate (2:1) to give **16** (420 mg, 84.0 %); ^{1}H NMR (300 MHz, $CDCl_3$) δ 8.39 - 8.31 (m, 1H), 8.09 - 8.00 (m, 1H), 7.76 - 7.65 (m, 1H), 7.58 - 7.51 (m, 1H), 7.47 (s, 1H), 2.78 (s, 3H), 2.71 (s, 3H); ^{13}C NMR (75 MHz, $CDCl_3$) δ 201.38,

158.40, 148.87, 143.07, 129.81, 129.16, 127.27, 125.22, 121.91, 120.70, 30.04, 25.34; ESI-MS *m/z* $[M+Na]^+$ 208.1.

1.3 2-Methylquinoline-4-carbaldehyde (19). Intermediate **18** was synthesized according to literature report.[40] To a solution of **18** (15.0 g, 86.7 mmol) in 50 mL CH_2Cl_2 was added Dess-Martin reagent (40.4 g, 95.3 mmol) in batches. The mixture was stirred for 2 h, and quenched by $Na_2S_2O_4$ aqueous. The residue was extracted with EtOAc (3 × 50 mL), and the combined organic layers were then washed with saturated $NaHCO_3$, brine, dried over anhydrous Na_2SO_4, and concentrated in vacuo to afford the crude product, which was purified by column chromatography with petroleum/ethyl acetate (2:1) to give **19** (12 g, 80.0 %); ^{1}H NMR (300 MHz, $CDCl_3$) δ 10.42 (s, 1H), 8.91 (d, J = 8.4 Hz, 1H), 8.09 (d, J = 8.5 Hz, 1H), 7.80 - 7.71 (m, 1H), 7.62 (d, J = 4.3 Hz, 2H), 2.83 (s, 3H); ^{13}C NMR (75 MHz, $CDCl_3$) δ 192.92, 159.09, 148.96, 136.96, 130.08, 129.15, 128.24, 127.06, 124.18, 122.15, 25.22; ESI-MS *m/z* $[M+Na]^+$ 194.1.

1.4 1-(2-Methylquinolin-4-yl)propan-1-one (21). A solution of C_2H_5MgBr in diethyl ether (3 M, 12 mL, 36.0 mmol) was added dropwise to a solution of **19** (5.0 g, 29.1 mmol) in 50 mL anhydrous THF under nitrogen atmosphere at 0 °C. After stirring for 2 h, the reaction was quenched by NH_4Cl aqueous, and extracted with CH_2Cl_2 (3 × 50 mL). The combined organic layers were then washed with brine, dried over anhydrous Na_2SO_4, and concentrated in vacuo to provide the crude product, which was purified by column chromatography with petroleum/ethyl acetate (2:1) to give intermediate **20** (4.3 g, 74.1 %). To a solution of **20** (2.0 g, 9.95 mmol) in 50 mL

CH_2Cl_2 was added Dess-Martin reagent (5.1 g, 11.9 mmol) in batches. The mixture was stirred for 2 h, and quenched by $Na_2S_2O_4$ aqueous. The residue extracted with EtOAc (3 × 50 mL), and the combined organic layers were then washed with saturated $NaHCO_3$, brine, dried over anhydrous Na_2SO_4, and concentrated in vacuo to afford the crude product, which was purified by column chromatography with petroleum/ethyl acetate (2:1) to give **21** (1.3 g, 65.1%). ^{1}H NMR (300 MHz, $CDCl_3$) δ 8.16 (d, J = 8.5 Hz, 1H), 8.03 (d, J = 8.5 Hz, 1H), 7.73 - 7.65 (m, 1H), 7.55 - 7.48 (m, 1H), 7.38 (s, 1H), 3.01 (q, J = 7.5 Hz, 2H), 2.76 (s, 3H), 1.25 (t, J = 7.2 Hz, 3H); ^{13}C NMR (75 MHz, $CDCl_3$) δ 158.38, 148.70, 144.14, 136.94, 129.85, 129.15, 127.08, 125.05, 122.09, 119.70, 35.85, 25.38, 8.05; ESI-MS *m/z* $[M+Na]^+$ 222.1.

1.5 General procedures for the preparation of 24a and 24b. To a solution of **16** (75 mg, 0.40 mmol) or **21** (80 mg, 0.40 mmol) in 5 mL EtOH was added NaOH (81 mg, 2.0 mmol). After stirring for 5 min, 3-nitro-4-methoxybenzaldehyde (88 mg, 0.49 mmol) was added in one portion. After reaction completed, the mixture was extracted with EtOAc (3 × 20 mL), and the combined organic layers were then washed with saturated brine, dried over anhydrous Na_2SO_4, and concentrated in vacuo to afford the crude products. The crude products were dissolved into the mixture solvent of 5 mL EtOH and 5 mL AcOH, Fe powder (77 mg, 1.38 mmol) was added, and the mixture was stirred at 65 °C for 30 min. Then, the solvent was removed in vacuo, and the residue was neutralized by saturated $NaHCO_3$ aqueous. The mixture was filtrated, and the filtrates was extracted with EtOAc (3 × 20 mL), and the combined organic layers were then washed with saturated brine, dried over anhydrous Na_2SO_4, and

concentrated in vacuo to afford the crude products, which was purified by column chromatography with petroleum/ethyl acetate (2:1) to give **24a** or **24b**.

(E)-3-(3-amino-4-methoxyphenyl)-1-(2-methylquinolin-4-yl)prop-2-en-1-one (24a). Yellow solid (54 mg, yield 42.5% over two steps).^{1}H NMR (300 MHz, $CDCl_3$) δ 8.07 (d, J = 8.5 Hz, 1H), 8.03 - 7.95 (m, 1H), 7.70 (ddd, J = 8.4, 6.8, 1.5 Hz, 1H), 7.51 - 7.45 (m, 1H), 7.37 (d, J = 17.0 Hz, 2H), 7.00 (d, J = 16.0 Hz, 1H), 6.94 - 6.85 (m, 2H), 6.75 (d, J = 8.2 Hz, 1H), 3.86 (s, 3H), 2.78 (s, 3H); ^{13}C NMR (75 MHz, CDCl3) δ 195.10, 158.43, 150.23, 148.66, 148.41, 145.59, 136.80, 129.86, 129.10, 127.11, 126.66, 125.24, 124.00, 123.01, 121.40, 119.94, 113.21, 110.21, 77.47, 77.05, 76.63, 55.62, 25.42; HR-MS (ESI) *m/z*: calcd for $C_{21}H_{21}N_2O_2$ $[M+H]^+$ 319.1441, found 319.1445; Purity: 95.2% (by HPLC).

(E)-3-(3-amino-4-methoxyphenyl)-2-methyl-1-(2-methylquinolin-4-yl)prop-2-en-1-one (24b). Yellow solid (65 mg, yield 50.4% over two steps). ^{1}H NMR (300 MHz, $CDCl_3$) δ 8.00 (d, J = 8.5 Hz, 1H), 7.64 (m, 2H), 7.39 (t, J = 7.4 Hz, 1H), 7.17 (d, J = 9.8 Hz, 1H), 6.97 (s, 1H), 6.84 - 6.56 (m, 3H), 3.79 (s, 3H), 2.70 (s, 3H), 2.28 (s, 3H); ^{13}C NMR (75 MHz, $CDCl_3$) δ 198.29, 157.71, 148.04, 147.56, 147.05, 146.18, 135.72, 134.76, 129.35, 128.50, 127.69, 125.95, 124.78, 123.32, 121.43, 119.44, 115.79, 109.56, 55.05, 29.17, 24.83; HR-MS (ESI) *m/z*: calcd for $C_{21}H_{21}N_2O_2$ $[M+H]^+$ 333.1598, found 333.1604. Purity: 98.2% (by HPLC).

1.6 General procedures for the preparation of 24c and 24d. To a solution of **16** (75 mg, 0.40 mmol) or **21** (80 mg, 0.40 mmol) in 5 mL EtOH was added NaOH (81 mg, 2.0 mmol). After stirring for 5 min, MEM protected isovanillin (117 mg, 0.49 mmol)

was added in one portion. After reaction completed, the mixture was extracted with EtOAc (3 × 20 mL), and the combined organic layers were then washed with saturated brine, dried over anhydrous Na_2SO_4, and concentrated in vacuo to afford the crude products, which was purified by column chromatography with petroleum/ethyl acetate (4:1) to give products as colorless oil. Then, the products were dissolved in 5 mL EtOH, 1 mL 10% HCl aqueous was added followed by refluxing for 30 min. Then, the mixture was extracted with EtOAc (3 × 20 mL), and the combined organic layers were then washed with saturated brine, dried over anhydrous Na_2SO_4, and concentrated in vacuo to afford the crude products, which was purified by column chromatography with petroleum/ethyl acetate (2:1) to give products **24c** or **24d**.

(E)-3-(3-hydroxy-4-methoxyphenyl)-1-(2-methylquinolin-4-yl)prop-2-en-1-one (24c). Yellow solid (65 mg, 50.3% over two steps). ^{1}H NMR (300 MHz, DMSO-d_6) δ 9.26 (s, 1H), 8.03 (d, J = 9.0 Hz, 2H), 7.76 (t, J = 7.6 Hz, 1H), 7.65 (s, 1H), 7.57 (t, J = 7.9 Hz, 1H), 7.50 (d, J = 16.0 Hz, 1H), 7.33 - 7.22 (m, 2H), 7.20 (d, J = 6.3 Hz, 1H), 6.97 (d, J = 8.4 Hz, 1H), 3.83 (s, 3H), 2.74 (s, 3H); ^{13}C NMR (75 MHz, DMSO-d_6) δ 193.80, 158.59, 150.87, 147.82, 147.55, 146.77, 144.27, 129.66, 128.80, 126.94, 126.61, 124.96, 123.60, 122.60, 122.37, 120.42, 114.68, 111.91, 55.65, 24.81; HR-MS (ESI) *m/z*: calcd for $C_{20}H_{18}NO_3$ $[M+H]^+$ 320.1281, found 320.1285. Purity: 95.8% (by HPLC).

(E)-3-(3-hydroxy-4-methoxyphenyl)-2-methyl-1-(2-methylquinolin-4-yl)prop-2-en-1-one (24d). Yellow solid (52 mg, 36.1% over two steps). ^{1}H NMR (300 MHz, $CDCl_3$) δ 8.08 (d, J = 8.5 Hz, 1H), 7.76 - 7.67 (m 2H), 7.47 (t, J = 7.6 Hz, 1H), 7.24 (s,

1H), 7.12 - 6.99 (m, 2H), 6.94 - 6.78 (m, 2H), 3.89 (s, 3H), 2.77 (s, 3H), 2.35 (s, 3H); ^{13}C NMR (75 MHz, $CDCl_3$) δ 198.19, 157.71, 147.54, 147.44, 146.36, 146.11, 145.21, 135.33, 129.44, 128.39, 128.07, 126.03, 124.75, 123.30, 123.06, 119.50, 115.76, 110.05, 76.94, 76.52, 76.10, 55.45, 24.71, 12.31; HR-MS (ESI) *m/z*: calcd for $C_{21}H_{20}NO_3$ $[M+H]^+$ 334.1438, found 334.1446. Purity: 99.3% (by HPLC).

1.7 General procedures for the preparation of 24e-h. To a solution of **16** (75 mg, 0.40 mmol) or **21** (80 mg, 0.40 mmol) in 5 mL EtOH was added NaOH (81 mg, 2.0 mmol). After stirring for 5 min, various benzaldehydes (0.49 mmol) was added in one portion. After reaction completed, the mixture was extracted with EtOAc (3 × 20 mL), and the combined organic layers were then washed with saturated brine, dried over anhydrous Na_2SO_4, and concentrated in vacuo to afford the crude products, which was purified by column chromatography with petroleum/ethyl acetate (2:1) to give **24e-h.**

(E)-3-(4-methoxyphenyl)-2-methyl-1-(2-methylquinolin-4-yl)prop-2-en-1-one (24e). White solid (82 mg, 64.4%). ^{1}H NMR (300 MHz, $CDCl_3$) δ 8.03 - 7.97 (m, 1H), 7.70 - 7.59 (m, 2H), 7.39 (m, 1H), 7.28 (s, 1H), 7.25 (s, 1H), 7.17 (s, 1H), 7.06 - 7.02 (m, 1H), 6.82 (d, J = 8.9 Hz, 2H), 3.74 (s, 3H), 2.71 (s, 3H), 2.29 (s, 3H).; ^{13}C NMR (75 MHz, $CDCl_3$) δ 198.20, 160.17, 157.71, 147.59, 146.21, 146.01, 134.96, 131.64, 129.37, 128.55, 127.27, 125.97, 124.73, 123.28, 119.42, 113.59, 54.85, 24.86, 12.35; HR-MS (ESI) *m/z*: calcd for $C_{21}H_{20}NO_2$ $[M+H]^+$ 318.1489, found 318.1494. Purity: 99.8% (by HPLC).

(E)-3-(3,4-dimethoxyphenyl)-2-methyl-1-(2-methylquinolin-4-yl)prop-2-en-1-one (24f). White solid (91 mg, 65.2%). ^{1}H NMR (300 MHz, $CDCl_3$) δ 8.04 - 7.97 (m,

1H), 7.70 - 7.59 (m, 2H), 7.44 - 7.36 (m, 1H), 7.18 (d, *J* = 7.1 Hz, 1H), 7.03 (d, *J* = 1.5 Hz, 1H), 6.95 (dd, *J* = 8.5, 2.0 Hz, 1H), 6.79 (dd, *J* = 5.3, 3.2 Hz, 2H), 3.82 (s, 3H), 3.76 (s, 3H), 2.70 (s, 3H), 2.31 (s, 3H); ^{13}C NMR (75 MHz, $CDCl_3$) δ 198.68, 158.25, 150.30, 148.75, 148.08, 146.94, 146.46, 135.66, 129.94, 129.02, 127.97, 126.53, 125.24, 124.13, 123.76, 119.93, 113.20, 110.88, 55.95, 25.42, 12.95; HR-MS (ESI) *m/z*: calcd for $C_{22}H_{12}NO_3$ $[M+H]^+$ 348.1594, found 348.1596. Purity: 99.6% (by HPLC).

(E)-3-(3-fluoro-4-methoxyphenyl)-2-methyl-1-(2-methylquinolin-4-yl)prop-2-en-1-one (24g). White solid (78 mg, 57.9%). ^{1}H NMR (300 MHz, $CDCl_3$) δ 8.08 (d, *J* = 8.5 Hz, 1H), 7.77 - 7.66 (m, 2H), 7.48 (m, 1H), 7.24 (s, 1H), 7.19 (dd, *J* = 12.4, 2.2 Hz, 1H), 7.10 - 7.03 (m, 2H), 6.93 (t, *J* = 8.5 Hz, 1H), 3.90 (s, 3H), 2.78 (s, 3H), 2.35 (s, 3H); ^{13}C NMR (75 MHz, $CDCl_3$) δ 198.01, 157.71, 147.62, 145.60, 144.66, 136.07, 129.42, 128.63, 127.71, 126.81, 126.04, 124.60, 123.17, 121.85, 119.42, 117.15, 116.90, 112.56, 55.73, 24.86, 12.31; HR-MS (ESI) *m/z*: calcd for $C_{21}H_{19}FNO_2$ $[M+H]^+$ 336.1394, found 336.1396. Purity: 95.1% (by HPLC).

(E)-2-methyl-1-(2-methylquinolin-4-yl)-3-(4-(methylthio)phenyl)prop-2-en-1-one (24h). White solid (83 mg, 62.0%). ^{1}H NMR (300 MHz, $CDCl_3$) δ 8.08 (d, *J* = 8.4 Hz, 1H), 7.79 - 7.66 (m, 2H), 7.49 (dd, *J* = 11.2, 4.0 Hz, 1H), 7.30 - 7.19 (m, 5H), 7.11 (s, 1H), 2.78 (s, 3H), 2.48 (s, 3H), 2.36 (s, 3H); ^{13}C NMR (75 MHz, $CDCl_3$) δ 198.72, 158.25, 148.09, 146.29, 146.24, 141.39, 136.77, 131.48, 130.62, 129.97, 129.08, 127.61, 126.80, 126.57, 125.59, 125.18, 123.72, 120.00, 25.40, 15.06, 12.99; HR-MS (ESI) *m/z*: calcd for $C_{21}H_{20}NOS$ $[M+H]^+$ 334.1260, found 334.1259. Purity:

98.2% (by HPLC).

1.8 General procedures for the preparation of 24i-o. To a solution of **16** (75 mg, 0.40 mmol) or **21** (80 mg, 0.40 mmol) in 5 mL EtOH, piperidine (48 μL, 0.48 mmol) and indole formaldehydes (0.48 mmol) were added. After the mixture was stirred at 95 °C for 48 h. After reaction completed, the mixture was extracted with EtOAc (3 × 20 mL), and the combined organic layers were then washed with saturated brine, dried over anhydrous Na_2SO_4, and concentrated in vacuo to afford the crude products, which was purified by column chromatography with petroleum/ethyl acetate (2:1) to give **24i-o.**

(E)-3-(1H-indol-4-yl)-1-(2-methylquinolin-4-yl)prop-2-en-1-one (24i). Yellow solid (74 mg, 54.9%). ^{1}H NMR (300 MHz, $CDCl_3$) δ 9.11 (s, 1H), 8.11 (dd, J = 8.2, 4.6 Hz, 2H), 7.97 (d, J = 16.1 Hz, 1H), 7.78 - 7.66 (m, 1H), 7.53 (d, J = 7.1 Hz, 1H), 7.48 (d, J = 3.4 Hz, 1H), 7.44 (m, 2H), 7.38 (s, 1H), 7.35 - 7.27 (m, 1H), 7.19 (t, J = 7.8 Hz, 1H), 6.74 (s, 1H), 2.81 (s, 3H); ^{13}C NMR (75 MHz, $CDCl_3$) δ 194.81, 157.99, 150.12, 147.86, 145.39, 137.27, 129.45, 128.47, 127.86, 126.21, 125.54, 125.26, 124.82, 123.19, 122.63, 121.49, 119.49, 111.40, 103.12, 76.96, 76.54, 76.12, 24.83; HR-MS (ESI) *m/z*: calcd for $C_{21}H_{17}N_2O$ $[M+H]^+$ 313.1335, found 313.1333. Purity: 97.2% (by HPLC).

(E)-3-(1H-indol-4-yl)-2-methyl-1-(2-methylquinolin-4-yl)prop-2-en-1-one (24j). Yellow solid (69 mg, 51.1%). ^{1}H NMR (300 MHz, $CDCl_3$) δ 8.71 (s, 1H), 8.02 (d, J = 8.4 Hz, 1H), 7.78 (d, J = 8.3 Hz, 1H), 7.63 (t, J = 7.1 Hz, 1H), 7.55 (s, 1H), 7.42 (t, J = 7.4 Hz, 1H), 7.29 (d, J = 8.0 Hz, 1H), 7.26 (s, 1H), 7.22 (d, J = 7.3 Hz, 1H), 7.14

(dd, J = 13.3, 5.6 Hz, 1H), 7.08 - 7.01 (m, 1H), 5.94 (s, 1H), 2.71 (s, 3H), 2.31 (s, 3H); ^{13}C NMR (75 MHz, $CDCl_3$) δ 198.58, 157.80, 147.58, 146.13, 144.91, 136.89, 135.29, 129.49, 128.49, 127.27, 126.53, 126.08, 124.90, 124.67, 123.37, 121.20, 120.48, 119.68, 112.13, 100.22, 24.81, 12.79; HR-MS (ESI) *m/z*: calcd for $C_{22}H_{19}N_2O$ $[M+H]^+$ 327.1492, found 327.1498. Purity: 96.6% (by HPLC).

(E)-3-(1H-indol-5-yl)-1-(2-methylquinolin-4-yl)prop-2-en-1-one (24k). Yellow solid (72 mg, 53.4%). ^{1}H NMR (300 MHz, $CDCl_3$) δ 8.87 (s, 1H), 8.02 (d, J = 8.5 Hz, 1H), 7.96 (d, J = 8.4 Hz, 1H), 7.72 (s, 1H), 7.66 - 7.56 (m, 2H), 7.43 (d, J = 7.4 Hz, 1H), 7.36 (m, 3H), 7.18 - 7.08 (m, 2H), 6.48 (s, 1H), 2.72 (s, 3H); ^{13}C NMR (75 MHz, $CDCl_3$) δ 194.83, 158.00, 150.13, 147.88, 145.41, 137.28, 129.46, 128.48, 127.87, 126.23, 125.55, 125.27, 124.83, 123.20, 122.64, 121.50, 119.50, 111.41, 103.13, 24.83; HR-MS (ESI) *m/z*: calcd for $C_{21}H_{17}N_2O$ $[M+H]^+$ 313.1335 found 313.1339. Purity: 96.4% (by HPLC).

(E)-3-(1H-indol-5-yl)-2-methyl-1-(2-methylquinolin-4-yl)prop-2-en-1-one (24l). Yellow solid (65 mg, 49.6%). ^{1}H NMR (300 MHz, $CDCl_3$) δ 8.98 (s, 1H), 8.09 (d, J = 8.4 Hz, 1H), 7.79 (d, J = 8.3 Hz, 1H), 7.72 (s, 1H), 7.67 (d, J = 7.2 Hz, 1H), 7.46 (t, J = 7.2 Hz, 1H), 7.38 - 7.24 (m, 3H), 7.19 (d, J = 7.6 Hz, 2H), 6.54 (s, 1H), 2.78 (s, 3H), 2.45 (s, 3H); ^{13}C NMR (75 MHz, $CDCl_3$) δ 198.53, 157.80, 148.99, 147.57, 146.47, 135.92, 134.36, 129.44, 128.41, 127.60, 126.46, 126.03, 125.11, 124.89, 124.17, 123.43, 123.37, 119.52, 110.76, 102.84, 24.81, 12.51; HR-MS (ESI) *m/z*: calcd for $C_{22}H_{19}N_2O$ $[M+H]^+$ 327.1492, found 327.1497. Purity: 95.1% (by HPLC).

(E)-2-methyl-3-(1-methyl-1H-indol-5-yl)-1-(2-methylquinolin-4-yl)prop-2-en-1-

one (24m). Yellow solid (78 mg, 57.1%). ^{1}H NMR (300 MHz, $CDCl_3$) δ 7.98 (d, J = 8.5 Hz, 1H), 7.72 - 7.65 (m, 1H), 7.62 - 7.53 (m, 2H), 7.35 (td, J = 7.0, 3.5 Hz, 1H), 7.24 (s, 1H), 7.19 - 7.09 (m, 3H), 6.93 (d, J = 3.1 Hz, 1H), 6.37 (d, J = 3.1 Hz, 1H), 3.62 (s, 3H), 2.67 (s, 3H), 2.38 - 2.30 (s, 3H); ^{13}C NMR (75 MHz, $CDCl_3$) δ 198.88, 158.25, 149.37, 148.12, 146.89, 137.11, 134.75, 130.19, 129.83, 129.05, 128.55, 126.52, 126.43, 125.39, 124.32, 124.07, 123.91, 119.98, 109.37, 102.05, 32.93, 25.43, 13.06; HR-MS (ESI) *m/z*: calcd for $C_{23}H_{21}N_2O$ $[M+H]^+$ 341.1648, found 341.1654. Purity: 97.1% (by HPLC).

(E)-3-(6-methoxy-1H-indol-3-yl)-1-(2-methylquinolin-4-yl)prop-2-en-1-one (24n). Yellow solid (65 mg, 46.9%). ^{1}H NMR (300 MHz, DMSO-d_6) δ 8.04 (s, 1H), 8.01 (s, 2H), 7.81 (d, J = 15.8 Hz, 1H), 7.75 (d, J = 7.2 Hz, 1H), 7.63 -7.52 (m, 2H), 7.41 (d, J = 9.1 Hz, 2H), 7.18 (d, J = 16.0 Hz, 1H), 6.90 (dd, J = 8.7, 2.1 Hz, 1H), 3.83 (s, 3H), 2.75 (s, 3H); ^{13}C NMR (75 MHz, DMSO-d_6) δ 193.73, 158.57, 155.16, 147.78, 145.56, 142.60, 134.44, 132.52, 129.60, 128.75, 126.37, 125.67, 125.14, 122.73, 119.95, 119.67, 113.32, 112.42, 112.17, 102.59, 55.53, 24.85; HR-MS (ESI) *m/z*: calcd for $C_{22}H_{19}N_2O_2$ $[M+H]^+$ 343.1441, found 343.1444. Purity: 96.0% (by HPLC).

(E)-3-(6-methoxy-1H-indol-3-yl)-2-methyl-1-(2-methylquinolin-4-yl)prop-2-en-1-one (24o). Yellow solid (59 mg, 41.2%). ^{1}H NMR (300 MHz, DMSO-d_6) δ 11.88 (s, 1H), 8.04 (d, J = 8.4 Hz, 1H), 7.88 (s, 1H), 7.81 - 7.67 (m, 2H), 7.52 (td, J = 6.8, 3.3 Hz, 1H), 7.44 (d, J = 6.9 Hz, 2H), 6.99 - 6.90 (m, 2H), 6.64 (dd, J = 8.7, 2.3 Hz, 1H), 3.74 (s, 3H), 2.74 (s, 3H), 2.31 (s, 3H); ^{13}C NMR (75 MHz, DMSO-d_6) δ 196.21,

158.25, 156.37, 147.41, 146.46, 138.33, 136.59, 130.38, 129.65, 128.77, 126.23, 125.11, 123.39, 121.06, 119.69, 118.10, 118.09, 111.33, 110.72, 94.96, 55.15, 40.34, 40.06, 39.79, 39.51, 39.23, 38.95, 38.67, 24.85, 13.16; HR-MS (ESI) *m/z*: calcd for $C_{23}H_{21}N_2O_2$ $[M+H]^+$ 357.1598, found 357.1595. Purity: 97.5% (by HPLC).

1.9 1-(2-(Hydroxymethyl)quinolin-4-yl)propan-1-one (28). To a solution of **21** (300 mg, 1.52 mmol) in 15 mL anhydrous CH_2Cl_2 was added *m*-CPBA (75%, 450 mg, 1.98 mmol) in one portion. The mixture was stirred for 2 h at ambient temperature. Then, the reaction was quenched by $Na_2S_2O_4$ aqueous. The residue was extracted with EtOAc (3 × 20 mL), and the combined organic layers were then washed with saturated $NaHCO_3$, brine, dried over anhydrous Na_2SO_4, and concentrated in vacuo to afford the crude product **27**. **27** was then dissolved in 20 mL Ac_2O, and the mixture was stirred at refluxing temperature for 2 h. After reaction completion, Ac_2O was removed in vacuo, and the residue was dissolved in 5 mL CH_3OH followed by the addition of ammonia in CH_3OH. After stirring for 30 min, solvent was removed in vacuo to afford the crude produce **28**, which was purified by column chromatography with petroleum/ethyl acetate (2:1) to give **28** as a yellow solid (200 mg, yield 67.9% over three steps).

1.10 General procedures for the preparation of 29a and 29c-n. The synthesis of **29a** and **29c-n** referred to the general procedures for the preparation of **24c** and **24d**.

(E)-3-(3-hydroxy-4-methoxyphenyl)-1-(2-(hydroxymethyl)quinolin-4-yl)-2-methylprop-2-en-1-one (29a). Yellow solid (61 mg, 43.7% over two steps). ^{1}H NMR (300 MHz, $CDCl_3$) δ 8.07 (d, J = 8.5 Hz, 1H), 7.69 (dd, J = 12.7, 8.4 Hz, 2H), 7.51 -

7.42 (m, 1H), 7.20 (d, *J* = 1.5 Hz, 1H), 6.97 (s, 2H), 6.75 (d, *J* = 8.7 Hz, 2H), 4.88 (s, 2H), 4.69 (s, 1H), 3.83 (s, 3H), 2.29 (s, 3H); ^{13}C NMR (75 MHz, $CDCl_3$) δ 198.49, 158.39, 147.89, 147.17, 147.08, 145.54, 135.77, 130.31, 129.04, 128.46, 127.19, 125.49, 124.95, 124.02, 123.80, 116.48, 116.09, 110.42, 64.26, 55.98, 29.70; HR-MS (ESI) *m/z*: calcd for $C_{21}H_{20}NO_4$ $[M+H]^+$ 350.1387, found 350.1381. Purity: 95.4% (by HPLC).

(E)-4-(3-(3-hydroxy-4-methoxyphenyl)-2-methylacryloyl)quinoline-2-carbaldehyde (29b). To a solution of **29a** (30 mg, 0.08 mmol) in 2 mL DMSO was added IBX (29 mg, 0.10 mmol). The reactions were stirred for 30 min, then the mixtures were diluted with 50 mL EtOAc, then washed with water (20 mL × 3), saturated brine, dried over anhydrous Na_2SO_4, and concentrated in vacuo to afford crude products, which was purified by column chromatography with petroleum/ethyl acetate (2:1) to give **29b** as yellow solid (26 mg, 74.9%). ^{1}H NMR (300 MHz, $CDCl_3$) δ 10.18 (s, 1H), 8.25 (d, *J* = 8.4 Hz, 1H), 7.90 (s, 1H), 7.86 - 7.73 (m, 2H), 7.62 (dd, *J* = 11.2, 4.1 Hz, 1H), 6.95 (s, 2H), 6.77 - 6.72 (m, 2H), 5.71 (s, 1H), 3.82 (s, 3H), 2.30 (s, 3H); ^{13}C NMR (75 MHz, $CDCl_3$) δ 197.83, 193.27, 151.69, 148.23, 147.93, 147.63, 147.40, 145.51, 135.73, 130.92, 130.88, 130.06, 128.35, 127.37, 125.71, 123.87, 116.10, 115.47, 110.40, 55.97, 29.70; HR-MS (ESI) *m/z*: calcd for $C_{21}H_{18}NO_4$ $[M+H]^+$ 348.1230, found 348.1232. Purity: 97.8% (by HPLC).

(E)-1-(2-chloroquinolin-4-yl)-3-(3-hydroxy-4-methoxyphenyl)-2-methylprop-2-en-1-one (29c). White solid (65 mg, 45.9% over two steps). ^{1}H NMR (300 MHz, $CDCl_3$) δ 8.01 (d, *J* = 8.4 Hz, 1H), 7.78 - 7.63 (m, 2H), 7.48 (t, *J* = 7.6 Hz, 1H), 7.28

(s, 1H), 7.00 (s, 2H), 6.86 - 6.72 (m, 2H), 5.67 (s, 1H), 3.84 (s, 3H), 2.29 (s, 3H); ^{13}C NMR (75 MHz, $CDCl_3$) δ 196.88, 149.93, 149.39, 148.15, 148.00, 147.59, 145.54, 135.55, 131.07, 129.01, 128.31, 127.74, 125.49, 124.36, 124.01, 120.21, 116.07, 110.42, 56.00, 29.70; HR-MS (ESI) *m/z*: calcd for $C_{20}H_{17}ClNO_3$ $[M+H]^+$ 354.0891, found 327.0895. Purity: 95.8% (by HPLC).

(E)-1-(2-(dimethylamino)quinolin-4-yl)-3-(3-hydroxy-4-methoxyphenyl)-2-methylprop-2-en-1-one (29d). Yellow solid (82 mg, 56.6% over two steps). ^{1}H NMR (300 MHz, DMSO-d_6) δ 9.16 (s, 1H), 7.53 (d, J = 8.1 Hz, 1H), 7.49 - 7.36 (m, 1H), 7.32 (d, J = 7.9 Hz, 1H), 7.07 (d, J = 7.3 Hz, 1H), 7.02 (s, 1H), 6.96 (s, 1H), 6.90 (s, 1H), 6.82 (dd, J = 16.2, 8.1 Hz, 2H), 3.69 (s, 3H), 3.08 (s, 6H), 2.17 (s, 3H); ^{13}C NMR (75 MHz, DMSO-d_6) δ 198.74, 156.79, 149.64, 148.20, 147.51, 146.81, 146.47, 134.80, 130.14, 128.04, 126.84, 125.25, 123.62, 122.32, 119.77, 117.40, 112.34, 107.92, 56.01, 38.13, 13.07; HR-MS (ESI) *m/z*: calcd for $C_{22}H_{23}N_2O_3$ $[M+H]^+$ 363.1703, found 363.1706. Purity: 96.4% (by HPLC).

(E)-3-(3-hydroxy-4-methoxyphenyl)-2-methyl-1-(2-(pyrrolidin-1-yl)quinolin-4-yl)prop-2-en-1-one (29e). Yellow solid (88 mg, 56.6% over two steps). ^{1}H NMR (300 MHz, $CDCl_3$) δ 7.76 (d, J = 8.5 Hz, 1H), 7.61 - 7.49 (m, 2H), 7.18 (s, 1H), 7.16 - 7.07 (m, 1H), 7.05 (s, 1H), 6.85 (q, J = 8.2 Hz, 2H), 6.66 (s, 1H), 3.89 (s, 3H), 3.62 (s, 4H), 2.32 (s, 3H), 2.03 (s, 4H); ^{13}C NMR (75 MHz, $CDCl_3$) δ 199.38, 154.69, 148.62, 147.99, 147.51, 146.68, 145.65, 135.59, 129.97, 128.67, 126.23, 125.28, 123.65, 121.95, 119.99, 116.25, 110.52, 108.61, 55.94, 47.00, 25.53, 12.79; HR-MS (ESI) *m/z*: calcd for $C_{24}H_{25}N_2O_3$ $[M+H]^+$ 389.1860, found 389.1868. Purity: 99.4% (by HPLC).

(E)-3-(3-hydroxy-4-methoxyphenyl)-2-methyl-1-(2-morpholinoquinolin-4-yl)prop-2-en-1-one (29f). Yellow solid (98 mg, 60.6% over two steps). ^{1}H NMR (300 MHz, $CDCl_3$) δ 7.76 (d, J = 8.3 Hz, 1H), 7.59 -7.53 (m, 2H), 7.22 (t, J = 7.5 Hz, 1H), 7.13 (s, 1H), 7.05 (s, 1H), 6.90 (s, 1H), 6.89 - 6.80 (m, 2H), 5.68 (s, 1H), 3.91 (s, 3H), 3.85 (d, J = 5.1 Hz, 4H), 3.73 (d, J = 5.1 Hz, 4H), 2.34 (s, 3H); ^{13}C NMR (75 MHz, $CDCl_3$) δ 199.17, 156.49, 148.11, 147.97, 147.78, 146.78, 145.49, 135.67, 130.12, 128.65, 127.11, 125.14, 123.75, 123.29, 120.70, 116.08, 110.42, 107.50, 66.82, 55.97, 45.48, 12.83; HR-MS (ESI) *m/z*: calcd for $C_{24}H_{25}N_2O_4$ $[M+H]^+$ 405.1809, found 405.1810. Purity: 96.5% (by HPLC).

(E)-3-(3-hydroxy-4-methoxyphenyl)-2-methyl-1-(2-(methylamino)quinolin-4-yl)prop-2-en-1-one (29g). Yellow solid (56 mg, 40.2% over two steps). ^{1}H NMR (300 MHz, $CDCl_3$) δ 7.75 (dt, J = 8.2, 1.3 Hz, 1H), 7.53 (dd, J = 8.9, 7.6 Hz, 2H), 7.21 - 7.13 (m, 2H), 7.04 (d, J = 2.0 Hz, 1H), 6.92 - 6.81 (m, 2H), 6.59 (s, 1H), 5.35 (s, 1H), 3.89 (s, 3H), 3.06 (s, 3H), 2.31 (s, 3H); ^{13}C NMR (75 MHz, $CDCl_3$) δ 198.80, 156.52, 148.06, 147.65, 146.83, 145.66, 135.48, 130.24, 128.57, 125.88, 125.35, 123.67, 122.72, 120.65, 116.29, 110.54, 109.13, 55.95, 28.79, 12.78; HR-MS (ESI) *m/z*: calcd for $C_{21}H_{21}N_2O_3$ $[M+H]^+$ 349.1547, found 327.1555. Purity: 96.0% (by HPLC).

(E)-1-(2-(ethylamino)quinolin-4-yl)-3-(3-hydroxy-4-methoxyphenyl)-2-methylprop-2-en-1-one (29h). Yellow solid (63 mg, 43.5% over two steps). ^{1}H NMR (300 MHz, $CDCl_3$) δ 7.72 (d, J = 8.5 Hz, 1H), 7.64 - 7.49 (m, 2H), 7.18 - 7.14 (m, 2H), 7.04 (d, J = 1.8 Hz, 1H), 6.90 (dd, J = 8.5, 1.7 Hz, 1H), 6.84 (d, J = 8.4 Hz, 1H), 6.58 (s, 1H), 4.90 (s, 1H), 3.89 (s, 3H), 3.60 - 3.48 (m, 2H), 2.31 (s, 3H), 1.27 (m, 3H); ^{13}C

NMR (75 MHz, $CDCl_3$) δ 198.94, 155.95, 148.10, 147.90, 146.74, 145.68, 135.52, 130.12, 128.61, 126.19, 125.32, 123.63, 122.62, 120.77, 116.34, 110.57, 109.21, 55.95, 36.67, 29.70, 14.95; HR-MS (ESI) *m/z*: calcd for $C_{22}H_{23}N_2O_3$ $[M+H]^+$ 363.1703, found 363.1702. Purity: 96.8% (by HPLC).

(E)-1-(2-(cyclopropylamino)quinolin-4-yl)-3-(3-hydroxy-4-methoxyphenyl)-2-methylprop-2-en-1-one (29i). Yellow solid (55 mg, 36.7% over two steps). ^1H NMR (300 MHz, $CDCl_3$) δ 7.62 (d, J = 8.5 Hz, 1H), 7.49 - 7.43 (m, 2H), 7.19 - 7.12 (m, 1H), 7.10 (s, 1H), 6.95 (s, 2H), 6.90 - 6.83 (m, 1H), 6.79 (d, J = 8.5 Hz, 1H), 5.47 (s, 1H), 3.84 (s, 3H), 2.62 - 2.49 (m, 1H), 2.28 (s, 3H), 1.18 (s, 4H); ^{13}C NMR (75 MHz, $CDCl_3$) δ 198.98, 176.06, 157.43, 147.79, 146.86, 145.75, 135.56, 130.27, 128.62, 125.99, 125.40, 123.51, 122.95, 121.10, 116.45, 115.52, 110.60, 107.84, 55.96, 29.70, 24.01, 12.82; HR-MS (ESI) *m/z*: calcd for $C_{23}H_{23}N_2O_3$ $[M+H]^+$ 375.1703, found 327.1709. Purity: 96.4% (by HPLC).

(E)-3-(3-hydroxy-4-methoxyphenyl)-1-(2-((4-methoxybenzyl)amino)quinolin-4-yl)-2-methylprop-2-en-1-one (29j). Yellow solid (103 mg, 56.7% over two steps). ^1H NMR (300 MHz, $CDCl_3$) δ 7.68 (d, J = 8.4 Hz, 1H), 7.51 - 7.40 (m, 2H), 7.23 - 7.18 (s, 2H), 7.10 (dd, J = 11.3, 3.8 Hz, 1H), 7.05 (s, 1H), 6.93 (s, 1H), 6.77 - 6.74 (m, 4H), 6.49 (s, 1H), 5.14 (s, 1H), 4.54 (s, 2H), 3.79 (s, 3H), 3.68 (s, 3H), 2.20 (s, 3H); ^{13}C NMR (75 MHz, $CDCl_3$) δ 198.83, 158.93, 155.68, 148.14, 147.94, 147.77, 146.70, 145.57, 135.53, 130.93, 130.12, 129.09, 128.61, 126.47, 125.32, 123.71, 122.81, 120.96, 116.24, 114.09, 110.50, 109.59, 55.94, 55.29, 45.40, 29.71; HR-MS (ESI) *m/z*: calcd for $C_{28}H_{27}N_2O_4$ $[M+H]^+$ 455.1965, found 455.1969. Purity: 95.8% (by HPLC).

(E)-3-(3-hydroxy-4-methoxyphenyl)-1-(2-methoxyquinolin-4-yl)-2-methylprop-2-en-1-one (29k). Yellow solid (88 mg, 63.0% over two steps). ^{1}H NMR (300 MHz, $CDCl_3$) δ 7.90 (d, J = 8.4 Hz, 1H), 7.68 - 7.62 (m, 2H), 7.42 - 7.31 (m, 1H), 7.14 (s, 1H), 7.05 (d, J = 1.8 Hz, 1H), 6.91 - 6.77 (m, 3H), 5.62 (s, 1H), 4.11 (s, 3H), 3.91 (s, 3H), 2.34 (s, 3H); ^{13}C NMR (75 MHz, $CDCl_3$) δ 198.27, 161.47, 148.94, 147.76, 146.93, 146.85, 145.45, 135.63, 130.00, 128.58, 127.63, 125.35, 124.67, 123.76, 122.59, 116.09, 111.41, 110.38, 55.95, 53.64, 12.83; HR-MS (ESI) *m/z*: calcd for $C_{21}H_{20}NO_4$ $[M+H]^+$ 350.1387, found 350.1392. Purity: 96.0% (by HPLC).

(E)-3-(3-hydroxy-4-methoxyphenyl)-2-methyl-1-(quinolin-4-yl)prop-2-en-1-one (29l). White solid (92 mg, 72.0% over two steps). ^{1}H NMR (300 MHz, $CDCl_3$) δ 8.88 (d, J = 4.3 Hz, 1H), 8.11 (d, J = 8.5 Hz, 1H), 7.73 (d, J = 8.0 Hz, 1H), 7.66 (dd, J = 11.2, 4.1 Hz, 1H), 7.47 (dd, J = 11.2, 4.0 Hz, 1H), 7.28 (d, J = 4.3 Hz, 1H), 7.00 - 6.90 (m, 2H), 6.82 - 6.74 (m, 2H), 3.80 (s, 3H), 2.28 (s, 3H); ^{13}C NMR (75 MHz, $CDCl_3$) δ 198.44, 149.27, 148.30, 148.14, 147.22, 146.51, 145.86, 135.69, 130.09, 129.57, 128.40, 127.57, 125.53, 123.62, 119.20, 116.43, 110.61, 55.94, 29.70; HR-MS (ESI) *m/z*: calcd for $C_{20}H_{18}NO_3$ $[M+H]^+$ 320.1281, found 320.1286. Purity: 98.2% (by HPLC).

(E)-4-(3-(3-hydroxy-4-methoxyphenyl)-2-methylacryloyl)quinolin-2(1H)-one (29m). Yellow solid (72 mg, 53.7% over two steps). ^{1}H NMR (300 MHz, $CDCl_3$) δ 12.71 (s, 1H), 7.44 (s, 2H), 7.39 (d, J = 8.2 Hz, 1H), 7.23 (s, 1H), 7.12 (s, 1H), 7.02 (s, 1H), 6.84 (d, J = 7.8 Hz, 1H), 6.76 (d, J = 8.1 Hz, 1H), 6.62 (s, 1H), 6.13 (s, 1H), 3.81 (s, 3H), 2.24 (s, 3H); ^{13}C NMR (75 MHz, $CDCl_3$) δ 197.04, 163.73, 151.34, 148.13,

147.27, 145.59, 138.70, 134.95, 131.36, 128.37, 126.12, 124.05, 123.28, 119.17, 118.02, 116.77, 116.31, 110.52, 55.97, 29.70; HR-MS (ESI) *m/z*: calcd for $C_{20}H_{18}NO_4[M+H]^+$ 336.1230, found 336.1233. Purity: 92.5% (by HPLC).

Ethyl(E)-4-(3-(3-hydroxy-4-methoxyphenyl)-2-methylacryloyl)quinoline-2-carboxylate(29n). Yellow solid (82 mg, 52.4% over two steps). ^{1}H NMR (300 MHz, $CDCl_3$) δ 8.26 (d, J = 8.5 Hz, 1H), 8.04 (s, 1H), 7.73 - 7.64 (m, 2H), 7.54 (t, J = 8.1 Hz, 1H), 7.03 - 6.87 (m, 2H), 6.82 - 6.66 (m, 2H), 4.44 (q, J = 7.1 Hz, 2H), 3.75 (s, 3H), 2.27 (s, 3H), 1.36 (t, J = 7.1 Hz, 3H); ^{13}C NMR (75 MHz, $CDCl_3$) δ 197.89, 164.90, 148.16, 147.78, 147.61, 147.56, 147.38, 145.62, 135.55, 130.98, 130.67, 129.42, 128.28, 126.50, 125.28, 123.89, 119.03, 116.28, 110.50, 62.46, 55.90, 29.67, 14.30; HR-MS (ESI) *m/z*: calcd for $C_{23}H_{22}NO_5$ $[M+H]^+$ 392.1492, found 392.1493. Purity: 95.1% (by HPLC).

1.11 2-Chloroquinoline-4-carbaldehyde (34). Intermediate **33** was synthesized according to literature report [40]. **34** was then prepared as the same procedures of **19** with **33** (5.0 g, 25.8 mmol) and Dess-Martin oxidant (12.1 g, 28.4 mmol) as the reagents. White solid, 84.0%. ^{1}H NMR (300 MHz, $CDCl_3$) δ 10.46 (s, 1H), 8.94 (dd, J = 8.5, 1.5 Hz, 1H), 8.15 - 8.07 (m, 1H), 7.87 - 7.70 (m, 3H); ^{13}C NMR (75 MHz, $CDCl_3$) δ 191.10, 150.68, 149.20, 139.51, 131.30, 129.45, 129.10, 127.28, 124.49, 122.79; ESI-MS *m/z* $[M+Na]^+$ 214.0.

1.12 1-(2-Chloroquinolin-4-yl)propan-1-ol (35). 35 was prepared as the same procedures of **20**. Colorless oil, yield 72.9%. ^{1}H NMR (300 MHz, $CDCl_3$) δ 8.00 - 7.93 (m, 1H), 7.93 - 7.86 (m, 1H), 7.71 - 7.62 (m, 1H), 7.53 (s, 1H), 7.52 - 7.44 (m,

1H), 5.35 (dd, *J* = 7.7, 4.2 Hz, 1H), 3.05 (s, 1H), 1.99 - 1.76 (m, 2H), 1.04 (t, *J* = 7.4 Hz, 3H); ^{13}C NMR (75 MHz, $CDCl_3$) δ 153.88, 151.00, 147.89, 130.10, 129.13, 126.72, 124.24, 123.10, 118.83, 70.97, 31.19, 10.11; ESI-MS *m/z* $[M+Na]^+$ 244.1.

1.13 1-(2-Chloroquinolin-4-yl)propan-1-one (36). 36 was prepared as the same procedures of **21**. Yellow solid, yield 65.0%. ^{1}H NMR (300 MHz, $CDCl_3$) δ 8.19 (d, J = 8.2 Hz, 1H), 8.05 (d, *J* = 8.5 Hz, 1H), 7.81 - 7.72 (m, 1H), 7.64 - 7.56 (m, 1H), 7.51 (s, 1H), 3.02 (q, *J* = 7.2 Hz, 2H), 1.28 (t, *J* = 7.2 Hz, 3H); ^{13}C NMR (75 MHz, $CDCl_3$) δ 203.03, 150.07, 148.79, 146.79, 130.99, 129.05, 128.25, 125.36, 122.71, 120.24, 35.93, 7.88; ESI-MS *m/z* $[M+Na]^+$ 242.0.

1.14 General procedures for the preparation of 37a-c. To a solution of **36** (150 mg, 0.68 mml) in 2 mL EtOH in sealed tube was added secondary amines (3.4 mmol). The mixture was stirred at 80 °C for 6 h. Then, the mixture was concentrated in vacuo to afford the crude products, which was purified by column chromatography with petroleum/ethyl acetate (2:1) to give **37a-c** as yellow solids.

1-(2-(Dimethylamino)quinolin-4-yl)propan-1-one (37a). Yellow solid (135 mg, 86.5%). ^{1}HNMR (300 MHz, $CDCl_3$) δ 7.88 (d, *J* = 8.3 Hz, 1H), 7.74 (d, *J* = 8.5 Hz, 1H), 7.58 - 7.50 (m, 1H), 7.26 - 7.18 (m, 1H), 6.95 (s, 1H), 3.23 (s, 6H), 2.99 (q, *J* = 7.2 Hz, 2H), 1.27 (s, 3H); ^{13}C NMR (75 MHz, $CDCl_3$) δ 205.53, 156.66, 148.97, 146.30, 129.84, 126.93, 124.76, 122.63, 118.06, 106.85, 38.02, 36.08, 29.69; ESI-MS *m/z* $[M+Na]^+$ 251.1.

1-(2-(Pyrrolidin-1-yl)quinolin-4-yl)propan-1-one (37b). Yellow solid (142 mg, 81.8%). ^{1}H NMR (300 MHz, $CDCl_3$) δ 7.91 - 7.84 (m, 1H), 7.74 (d, *J* = 8.4 Hz, 1H),

7.58 - 7.50 (m, 1H), 7.20 (d, *J* = 7.7 Hz, 1H), 6.78 (s, 1H), 3.62 (s, 4H), 2.99 (q, *J* = 7.2 Hz, 2H), 2.05 (s, 4H), 1.27 (s, 3H); ^{13}C NMR (75 MHz, $CDCl_3$) δ 205.52, 154.79, 149.36, 146.05, 129.81, 126.73, 124.88, 122.26, 118.20, 108.08, 46.89, 36.09, 25.51, 8.10; ESI-MS *m/z* $[M+Na]^+$ 277.1.

1-(2-Morpholinoquinolin-4-yl)propan-1-one (37c). Yellow solid (164 mg, 88.8%). ^{1}H NMR (300 MHz, $CDCl_3$) δ 7.95 - 7.84 (m, 1H), 7.75 (d, *J* = 8.4 Hz, 1H), 7.64 - 7.53 (m, 1H), 7.33 - 7.24 (m, 1H), 7.03 (s, 1H), 3.86 (t, *J* = 4.8 Hz, 4H), 3.72 (t, *J* = 4.8 Hz, 4H), 2.99 (q, *J* = 7.2 Hz, 2H), 1.28 (t, *J* = 7.3 Hz, 3H); ^{13}C NMR (75 MHz, $CDCl_3$) δ 205.28, 156.59, 148.55, 146.72, 130.06, 127.31, 124.79, 123.70, 118.96, 107.15, 66.77, 45.59, 36.11, 8.06; ESI-MS *m/z* $[M+Na]^+$ 293.1.

1.15 General procedures for the preparation of 39a-d. To a solution of **35** (100 mg, 0.45 mmol) in 2 mL EtOH in sealed tube was added primary amines (4.5 mmol). The mixture was stirred at 150 °C for 2 d. Then, the mixture was concentrated in vacuo to afford the crude products **38a-d**. **38a-d** were dissolved in 5 mL DMSO, IBX (150 mg, 0.56 mmol) was added. The reactions were stirred for 30 min, then the mixtures were diluted with 50 mL EtOAc, then washed with water (20 mL × 3), saturated brine, dried over anhydrous Na_2SO_4, and concentrated in vacuo to afford crude products, which was purified by column chromatography with petroleum/ethyl acetate (2:1) to give **39a-d**.

1-(2-(Methylamino)quinolin-4-yl)propan-1-one (39a). Colorless oil (55 mg, 56.9%). ^{1}H NMR (300 MHz, $CDCl_3$) δ 7.96 - 7.86 (m, 1H), 7.74 (d, *J* = 8.4 Hz, 1H), 7.56 (m, 1H), 7.30 - 7.19 (m, 1H), 6.71 (s, 1H), 5.00 (s, 1H), 3.09 (d, *J* = 4.4 Hz, 3H),

2.94 (q, J = 7.3 Hz, 2H), 1.25 (t, J = 7.2 Hz, 3H); ^{13}C NMR (75 MHz, $CDCl_3$) δ 205.02, 156.61, 148.84, 146.08, 130.00, 126.64, 125.00, 123.00, 119.01, 109.49, 35.92, 28.65, 8.03; ESI-MS *m/z* $[M+Na]^+$ 237.1.

1-(2-(Ethylamino)quinolin-4-yl)propan-1-one (39b). Colorless oil (51 mg, 49.1%). ^{1}H NMR (300 MHz, $CDCl_3$) δ 7.90 (d, J = 8.2 Hz, 1H), 7.71 (d, J = 8.4 Hz, 1H), 7.55 (t, J = 7.7 Hz, 1H), 7.25 (d, J = 8.5 Hz, 1H), 6.71 (s, 1H), 4.80 (s, 1H), 3.56 (d, J = 6.6 Hz, 2H), 2.95 (d, J = 7.3 Hz, 2H), 1.36 - 1.19 (m, 6H); ^{13}C NMR (75 MHz, $CDCl_3$) δ 205.05, 155.97, 148.99, 146.05, 129.94, 126.73, 124.97, 122.94, 119.05, 109.52, 36.55, 35.91, 14.93, 8.05; ESI-MS *m/z* $[M+Na]^+$ 253.1.

1-(2-((4-Methoxybenzyl)amino)quinolin-4-yl)propan-1-one (39d). Colorless oil (65 mg, 45.0%). ^{1}H NMR (300 MHz, $CDCl_3$) δ 7.95 - 7.88 (m, 1H), 7.74 (d, J = 8.4 Hz, 1H), 7.60 - 7.50 (m, 1H), 7.30 (d, J = 8.2 Hz, 2H), 7.26 - 7.20 (m, 1H), 6.89 - 6.82 (m, 2H), 6.68 (s, 1H), 5.12 (d, J = 5.6 Hz, 1H), 4.64 (d, J = 5.4 Hz, 2H), 3.77 (s, 3H), 2.87 (d, J = 7.2 Hz, 2H), 1.24 - 1.13 (m, 3H); ^{13}C NMR (75 MHz, $CDCl_3$) δ 204.95, 158.98, 155.69, 148.89, 145.89, 131.08, 130.00, 129.19, 126.86, 125.04, 123.16, 119.24, 114.07, 109.99, 55.30, 45.29, 35.83, 8.06; ESI-MS *m/z* $[M+Na]^+$ 343.2.

1.16 4-Propionylquinoline-2-carbonitrile (40). To a solution of **36** (500 mg, 2.25 mmol) in 10 mL DMF was added $Ph_3(PPh_3)_4$ (260 mg, 0.25mmol), $Zn(CN)_2$ (320 mg, 2.7 mmol), the mixture was stirred at 120 °C for 2 h under nitrogen atmosphere. Then, the mixture was diluted with 50 mL EtOAc, washed with water (20 mL × 3), saturated brine, dried over anhydrous Na_2SO_4, and concentrated in vacuo to afford crude

products, which was purified by column chromatography with petroleum/ethyl acetate (30:1) to give **40** as a yellow solid (415 mg, 87.0%). ^{1}H NMR (300 MHz, $CDCl_3$) δ 8.21 (d, J = 8.5 Hz, 1H), 8.07 (d, J = 7.8 Hz, 1H), 7.82 - 7.75 (m, 1H), 7.66 - 7.59 (m, 1H), 7.53 (s, 1H), 3.04 (q, J = 7.6, 5.3 Hz, 2H), 1.28 (d, J = 6.3 Hz, 3H); ^{13}C NMR (75 MHz, $CDCl_3$) δ ^{13}C NMR (75 MHz, $CDCl_3$) δ 202.10, 182.78, 145.76, 132.51, 130.02, 128.06, 127.28, 124.36, 121.70, 120.13, 119.24, 34.95, 6.89; ESI-MS *m/z* $[M+Na]^+$ 211.1.

1.17 1-(2-Methoxyquinolin-4-yl)propan-1-one (41). To a solution of **36** (150 mg, 0.68 mml) in 10 mL CH_3OH was added CH_3ONa (180 mg, 3.4 mmol), the mixture was stirred at refluxing temperature under nitrogen atmosphere for 4 h. Then, the mixture was extracted with EtOAc (3 × 20 mL), and the combined organic layers were then washed with brine, dried over anhydrous Na_2SO_4, and concentrated in vacuo to afford the crude product, which was purified by column chromatography with petroleum/ethyl acetate (20:1) to give **41** as yellow solid (130 mg, 88.4%). ^{1}H NMR (300 MHz, $CDCl_3$) δ 8.17 - 8.08 (m, 1H), 7.93 - 7.85 (m, 1H), 7.70 - 7.61 (m, 1H), 7.47 - 7.38 (m, 1H), 7.06 (s, 1H), 4.10 (s, 3H), 3.00 (q, J = 7.2 Hz, 2H), 1.27 (t, J = 7.3 Hz, 3H); ^{13}C NMR (75 MHz, $CDCl_3$) δ 204.17, 161.61, 147.53, 146.82, 129.96, 127.73, 125.26, 125.11, 120.94, 111.68, 53.65, 35.72, 8.01; ESI-MS *m/z* $[M+Na]^+$ 238.1.

1.18 4-Propionylquinolin-2(1H)-one (42). To a solution of **36** (100 mg, 0.46 mmol) in the mixture solvent of H_2O (10 mL) and AcOH (2 mL) was added CH_3SO_2Na (92 mg, 0.92 mmol), the mixture was stirred at 90 °C overnight. Then, the mixture was

neutralized by saturated $NaHCO_3$ aqueous, and extracted with EtOAc (3 × 20 mL), and the combined organic layers were then washed with brine, dried over anhydrous Na_2SO_4, and concentrated in vacuo to afford the crude product, which was purified by column chromatography with petroleum/ethyl acetate (20:1) to give **42** as a white solid (80 mg, 87.3%). ^{1}H NMR (300 MHz, DMSO-d_6) δ 12.01 (s, 1H), 7.67 (d, J = 8.2 Hz, 1H), 7.58 - 7.51 (m, 1H), 7.38 (d, J = 8.2 Hz, 1H), 7.22 - 7.14 (m, 1H), 6.89 (s, 1H), 3.10 - 2.97 (m, 2H), 1.16 - 1.02 (m, 3H); ^{13}C NMR (75 MHz, DMSO-d_6) δ 204.19, 161.18, 148.22, 139.41, 130.77, 125.67, 122.11, 120.64, 115.75, 115.16, 35.14, 7.49; ESI-MS *m/z* $[M+Na]^+$ 224.1.

1.19 1-(Quinolin-4-yl)propan-1-one (45). 45 was prepared as the same procedures of **21** with the commercially available **43** (500 mg, 3.18 mmol) as the starting material. Colorless oil (320 mg, 54.3% over two steps). ^{1}H NMR (300 MHz, $CDCl_3$) δ 8.89 (d, J = 4.4 Hz, 1H), 8.21 (dd, J = 8.6, 1.4 Hz, 1H), 8.12 - 8.03 (m, 1H), 7.70 - 7.63 (m, 1H), 7.56 - 7.48 (m, 1H), 7.43 (d, J = 4.4 Hz, 1H), 2.95 (q, J = 7.2 Hz, 2H), 1.19 (t, J = 7.2 Hz, 3H); ^{13}C NMR (75 MHz, $CDCl_3$) δ 204.42, 149.65, 148.88, 143.56, 129.82, 129.76, 128.03, 125.27, 123.73, 118.82, 35.69, 7.97; ESI-MS *m/z* $[M+Na]^+$ 208.1.

2. Biology.

2.1 Materials. 3-(4,5-Dimethylthiazol-2-yl)-2,5-diphenyl-2-H-tetrazolium bromide (MTT), propidium iodide (PI), the Annexin V-FITC apoptosis detection kit, 5,5′,6,6′-tetrachloro-1,1′,3,3′-tetraethyl-imidacarbocyanine iodide (JC-1) were purchased from Nanjing KeyGen Biotech Co. Ltd. (Nanjing, China). Goat antimouse IgG/Alexa-Fluor 488 antibody was purchased from Jackson ImmunoResearch in USA.

Primary antibodies against cdc25c, cdc2, cyclin B1, Bax, Bad, Bcl-2 and Bcl-xl were purchased from Beyotime (Jiangsu, China). The purified tubulin polymerization kit was purchased from Cytoskeleton Inc. (Denver, USA). Other reagents were purchased from Sigma-Aldrich (St. Louis, MO, USA) unless otherwise specified.

2.2 Cell Lines and Cell Culture. Human chronic myelogenous leukemia cells (K562), hepatocellular carcinoma cells (HepG2), epidermoid carcinoma of the nasopharynx cells (KB), human colon cancer cells (HCT-8), and human breast cancer cells (MDA-MB-231) were grown in RPMI 1640 medium (KeyGen Biotech Co. Ltd., Nanjing, China). Human umbilical vein endothelial cells (HUVECs) were grown in F12K medium (KeyGen Biotech Co. Ltd., Nanjing, China). The medium for all cell lines were supplemented with 10% fetal bovine serum (Life Technologies, USA), 100 μg/mL streptomycin (Life Technologies, USA), and 100 U/mL penicillin (Life Technologies, USA) and maintained at 37 °C in a humidified atmosphere with 5% CO_2.

2.3 MTT Assay. The overall growth of human cancer cell lines was determined using the colorimetric MTT assay. Briefly, the cell lines were incubated at 37 °C in a humidified 5% CO_2 incubator for 24 h in 96-well plates prior to the experiments. K562, HepG2, KB, HCT-8, and MDA-MB-231 were seeded at a density of 5×10^3 cells/well. After removal of medium, 100 μL of fresh medium containing the test compound at different concentrations was added to each well and incubated at 37 °C for 24 or 72 h. The percentage of DMSO in the medium was not exceeded 0.25%. The number of living cells after 72 h (or 24 h) of culture in the presence (or absence:

control) of the various compounds is directly proportional to the intensity of the blue color of media, which is quantitatively measured by spectrophotometry (Biorad, Nazareth, Belgium) at a 570 nm wavelength. The experiment was performed in quadruplicate and repeated three times.

2.4 In Vitro Tubulin Polymerization Inhibitory Assay. The tubulin reaction mix in 100 μL PEM buffer contained 2 mg/mL tubulin (Cytoskeleton), 80 mM piperazine-N,N′-bis(2-ethanesulfonic acid) sequisodium salt PIPES (pH 6.9), 0.5 mM EGTA, 2 mM $MgCl_2$, and 15% glycerol. Then, the mixture was preincubated with compounds or vehicle DMSO on ice. PEG containing GTP was added to the final concentration of 3 mg/mL before detecting the tubulin polymerization reaction. After 30 min, the absorbance was detected by a spectrophotometer at 340 nm at 37 °C every 2 min for 60 min. The area under the curve was used to determine the concentration that inhibited tubulin polymerization by 50% (IC_{50}), which was calculated with GraphPad Prism Software version 5.02.

2.5 Competitive Inhibition Assays. The competitive binding activity of inhibitors was evaluated using a radiolabeled [3H]-colchicine competition scintillation proximity (SPA) assay. In brief, 0.08 μM [3H]-colchicine was mixed with **24d** (1 μM, 5 μM) or CA-4 (1 μM, 5 μM) and biotinylated porcine tubulin (0.5 μg) in a buffer of 100 μL containing 80 mM PIPES (pH 6.8), 1mM EGTA, 10% glycerol, 1mM $MgCl_2$, and 1mM GTP for 2 h at 37 °C. Then streptavidin-labeled SPA beads (80 μg) were added to each mixture. The radioactive counts were measured directly with a scintillation counter.

2.6 Immunofluorescent Staining. K562 cells were seeded into 6-well plates and then treated with vehicle control 0.1% DMSO, **24d** (5 nM, 10 nM, 20 nM). The cells were fixed with 4% paraformaldehyde and then washed with PBS for three times. After blocking for 20 min by adding 50-100 μL goat serum albumin at room temperature, cells were incubated with a monoclonal antibody (anti-α-tubulin) at 37 °C for 2 h. Then the cells were washed three times by PBS following staining by fluorescence secondary antibody and labeling of nuclei by 4,6-diamidino-2-phenylindole (DAPI). Cells were finally visualized on a Zeiss LSM 570 laser scanning confocal microscope (Carl Zeiss, Germany).

2.7 Molecular Modeling. In our study, the X-ray structure of CA-4-*α,β*-tubulin complex was downloaded from the Protein Data Bank (PDB code 5lyj). The protein was prepared by removal of the stathmin-like domain, subunits C and D, water molecules and CA-4 using Discovery Studio modules. The docking procedure was performed by employing DOCK program in Discovery Studio 3.0 software, and the structural image was obtained using PyMOL software.

2.8 Cell Cycle Analysis. K562 cells were seeded into 6-well plates and incubated at 37 °C in a humidified 5% CO_2 incubator for 24 h, and then treated with or without **24d** at indicated concentrations for another 48 h. The collected cells were fixed by adding 70% ethanol at 4 °C for 12 h. Subsequently, the cells were resuspended in PBS containing 100 mL RNase A and 400 mL of propidium iodide for 30 min. The DNA content of the cells was measured using a FACS Calibur flow cytometer (Bectone Dickinson, San Jose, CA, USA).

2.9 Hoechst 33342 Staining. Approximately 5×10^4 cells per well were plated in six-well plates, and the cells were then incubated with 0, 5, 10, and 20 nM **24d** for 48 h. After incubation, cells were washed with PBS, fixed in 4% paraformaldehyde for 30 min, and then stained with 20 μg/mL Hoechst 33342 for 15 min at room temperature in the dark. Cells were then assessed by fluorescence microscopy for morphological changes after **24d** treatment.

2.10 Cell Apoptosis Analysis. After treatment with or without **24d** at indicated concentrations for 48 h, the cells were washed twice in PBS, centrifuged and resuspended in 500 mL AnnexinV binding buffer. The cells were then harvested, washed and stained with 5 mL Annexin V-APC and 5 mL 7-AAD in the darkness for 15 min. Apoptosis was analyzed using a FACS Calibur flow cytometer (Bectone Dickinson, San Jose, CA, USA).

2.11 Mitochondrial Membrane Potential Analysis. After treatment with vehicle control 0.1% DMSO, **24d** (5 nM, 10 nM, and 20 nM) for 48 h, the cells were washed in PBS and resuspended in 500 μL JC-1 incubation buffer at 37 °C for 15 min. The percentage of cells with healthy or collapsed mitochondrial membrane potentials was monitored by flow cytometry analysis (Bectone-Dickinson, San Jose, CA, USA).

Measurement of Intracellular ROS Generation. Intracellular ROS production was detected by using the peroxide-sensitive fluorescent probe DCF-DA. In brief, after treatment with 0, 5, 10, and 20 nM **24d** for 48 h, the cells were incubated with 10 mM DCF-DA at 37 °C for 15 min. The intracellular ROS mediated oxidation of DCF-DA to the fluorescent compound 2′,7′-dichlorofluorescein (DCF). Then cells were

harvested, and the pellets were suspended in 1 mL PBS. Samples were analyzed at an excitation wavelength of 480 nm and an emission wavelength of 525 nm by flow cytometry on a FC500 cytometer (Beckman Coulter).

2.12 Transwell Migration and Invasion Assay. In the invasion assay, diluted Matrigel was added to the upper chamber whereas for migration assay, the chamber was not coated with Matrigel. MDB-MB231 cells (1×10^5 cells/well) were cultured in the upper chambers of 24-well transwell plates (8 μm pore, Corning Costar), and **24d** (0, 2, 5, and 10 nM) was treated on the lower surface for 48 h. The cells on the upper surface of the membrane were removed, and the migrated or invaded cells on the bottom surface of the membranes were stained with crystal violet. The images of migrated or invaded cells at the bottom part of the chamber were captured and the number of migrated or invaded cells determined by counting cells in at least three fields from random sites.

2.13 Wound Healing Assays. K562 cells were grown in 6-well plates for 24 h. Scratches were made in confluent monolayers using 200 μL pipette tips. Then, wounds were washed twice with PBS to remove non-adherent cell debris. The media containing different concentrations (0, 5, 10, and 20 nM) of **24d** were added to the petri dishes. Cells which migrated across the wound area were photographed using phase contrast microscopy at 0 h and 24 h. The migration distance of cells migrated in to the wound area was measured manually.

2.14 Tube Formation Assay. EC Matrigel matrix was thawed at 4 °C overnight, and HUVECs suspended in F12K were seeded in 96-well culture plates at a cell density of

50,000 cells/well after polymerization of the Matrigel at 37 °C for 30 min. They were then treated with 20 μL different concentrations of **24d** or vehicle for 6 h at 37 °C. Then, the morphological changes of the cells and tubes formed were observed and photographed under inverted microscope (OLYMPUS, Japan).

2.15 Solubility Evaluation. Compounds **1** and **24d** were added to phosphate buffer (50 mM, pH 7.4) at 20 °C. After shaking and centrifuging, the supernatant was taken to determine the concentration of compounds **1** and **24d** in each solvent for calculation of the corresponding solubility. The samples (10 μL each) were analyzed by HPLC (Shimadzu DGU-20A3R) on Shimadzu-GL WondaSil C18-WR column. The mobile phase was acetonitrile-water (70/30, v/v) at a flow rate of 1.0 mL/min with the detection wavelength at 254 nm. This experiment was repeated in triplicates.

2.16 Acute Toxicity Determination. Five-week-old male Institute of Cancer Research (ICR) mice were purchased from Shanghai SLAC Laboratory Animals Co. Ltd. An acute toxicity study by intravenous injection was conducted according to the guidelines of the Organization for Economic Co-operation and Development. The animals were weighed and at random divided into five groups of ten animals. Then, the mice were intravenous injected with **24d** (409.6, 512, 640, 800, and 1000 mg/kg) in a vehicle of 10% DMF/2% Tween 80/88% saline. The animals were observed continuously for 14 days.

2.17 In Vivo Anti-tumor Effect Evaluation. A total of 1×10^6 H22 cells were subcutaneously inoculated into the right flank of ICR mice according to protocols of tumor transplant research. After incubation for one day, mice were weighted and at

random divided into eight groups with eight animals per groups. The groups treated with **24d** and CA-4 were administered 10, 20 mg/kg in a vehicle of 10% DMF/2% Tween 80/88% saline, respectively. The groups treated with **24d-HCl** were administered 10, 20 mg/kg in a vehicle of saline. The positive control group was treated with PTX (8 mg/kg) every 2 days by intravenous injection. The negative control group received a vehicle of 10% DMF/2% Tween 80/88% saline through intravenous injection. Treatments of **24d, 24d-HCl** and CA-4 were conducted at a frequency of intravenous injection one dose per day for a total 21 consecutive days while the positive group was treated with PTX one dose per two days. Body weights and tumor volumes were measured every 2 days. After the treatments, all the mice were sacrificed and weighed. The following formula was used to determine tumor volumes: tumor volume = $L \times W^2/2$, where L is the length and W is the width. Ratio of inhibition of tumor (%) = (1 − average tumor weight of treated group/average tumor weight of control group) × 100%. All procedures were performed following institutional approval in accordance with the NIH Guide for the Care and Use of Laboratory Animals.

2.18 Immunohistochemistry assay. Slides from mouse tissues (**24d**-treated group at 20 mg/kg) were embedded in paraffin were cut to a section of 4 μm, deparaffinized, and treated with citrate buffer. Then, they were blocked with avidin/biotin for 20 min. The slides were incubated with CD31 overnight at 4 °C. Next, the slides were treated with secondary antibody with horseradish peroxidase goat anti-rabbit for 1-3 h and developed with 3, 3-diaminobenzidine. Finally, the slides were counterstained with

hematoxylin. The mean microvessel density (MVD) was measured by calculating the CD31-positive cells in randomly selected areas in each section using image analysis software and then analyzed with OriginPro 8.0 software.

SUPPORTING INFORMATION AVAILABLE

^{1}H and ^{13}C NMR spectra for key intermediates and all target compounds, HPLC trace for compound **24d** and Molecular Formula Strings are available free of charge via the internet at http://pubs.acs.org.

The statement for Molecular modeling (PDB) file: Authors will release the atomic coordinates and experimental data upon article publication.

AUTHOR INFORMATION

Corresponding Authors

*E-mail: jinyixu@china.com (J. Xu); cpuxst@163.com (S. Xu).

ORCID

Jinyi Xu: 0000-0002-1961-0402

Funding

This study was supported from the National Natural Science Foundation of China (No. 81673306, 81703348), The Open Project of State Key Laboratory of Natural Medicines, China Pharmaceutical University (No. SKLNMKF 201710), China Postdoctoral Science Foundation (No. 2017100424) for financial support, and "Double First-Class" University project CPU2018GY04, China Pharmaceutical University.

Notes

The authors declare no competing financial interest.

ABBREVIATIONS USED

CA-4, Combretastatin A-4; MEM, 2-Methoxyethoxymethyl chloride; *m*-CPBA, meta-chloroperoxybenzoic acid; DMAP, 4-dimethylaminopyridine; EDCI, 1-(3-(dimethylamino)propyl)-3-ethylcarbodiimide hydrochloride; HOBt, 1-hydroxybenzotriazole; DMF, dimethylformamide; DMSO, dimethyl sulfoxide; Ac_2O, acetic anhydride; $POCl_3$, phosphorus oxychloride; DCM, dichloromethane; THF, tetrahydrofuran; IBX, 2-iodoxybenzoic acid; MTT, 3-(4,5-dimethyl-2-thiazolyl)-2,5-diphenyl-2-Htetrazolium bromide; PI, propidium iodide; Dess-Martin reagent, 1,1,1-Triacetoxy-1,1-dihydro-1,2-benziodoxol-3(1H)-one; ROS, reactive oxidative stress.

REFERENCES

1. Stanton R. A.; Gernert K. M.; Nettles J. H.; Aneja R. Drugs that target dynamic microtubules: A new molecular perspective. *Med. Res. Rev*. **2011**, *31*, 443-481.
2. Howard J.; Hyman A. A. Dynamics and mechanics of the microtubule plus end. *Nature*. **2003**, *422*, 753-758.
3. Jordan M. A.; Wilson L. Microtubules as a target for anticancer drugs. *Nat. Rev. Cancer.* **2004**, *4*, 253-265.
4. Islam M. N.; Iskander M. N. Microtubulin binding sites as target for developing anticancer agents. *Mini-Rev. Med. Chem*. **2004**, *4*, 1077-1104.
5. Dumontet C.; Jordan M. A. Microtubule-binding agents: a dynamic field of cancer therapeutics. *Nat. Rev. Drug Discovery* **2010**, *9*, 790-803.
6. Pettit, G. R.; Singh, S. B.; Hamel, E.; Lin, C. M.; Alberts, D. S.; Garcia-Kendal,

D. Isolation and structure of the strong cell growth and tubulin inhibitor combretastatin A-4. *Experientia*. **1989**, *45*, 209-211.

7. Pettit, G. R.; Temple, J. C.; Narayanan, V. L.; Varma, R. A. V. I.; Simpson, M. J.; Boyd, M. R.; Bansal, N. A. M. I. T. A. Antineoplastic agents 322. Synthesis of combretastatin A-4 prodrugs. *Anti-Cancer Drug Des*. **1995**, *10*, 299-309.
8. Yakushiji, F.; Tanaka, H.; Muguruma, K.; Iwahashi, T.; Yamazaki, Y.; Hayashi, Y. Prodrug study of plinabulin using a click strategy focused on the effects of a replaceable water-solubilizing moiety. *Chem. Pharm. Bull*. **2012**, *60*, 877-881.
9. Sève P.; Dumontet C. Is class III beta-tubulin a predictive factor in patients receiving tubulin-binding agents? *Lancet Oncol*. **2008**, *9*, 168-175.
10. Stengel C.; Newman S. P.; Leese M. P.; Potter B. V.; Reed M. J.; Purohit A. Class III beta-tubulin expression and in vitro resistance to microtubule targeting agents. *Br. J. Cancer*. **2010**, *102*, 316-324.
11. Lu, Y.; Chen, J. J.; Xiao, M.; Li, W.; Miller, D. D. An overview of tubulin inhibitors that interact with the colchicine binding site. *Pharm. Res.* **2012**, *29*, 2943-2971.
12. Dong M.; Liu F.; Zhou H.; Zhai S.; Yan B. Novel natural product- and privileged scaffold-based tubulin inhibitors targeting the colchicine binding site. *Molecules.* **2016**, *21*, 1375-1400.
13. Porcù E.; Bortolozzi R.; Basso G.; Viola G. Recent advances in vascular disrupting agents in cancer therapy. *Future Med. Chem*. **2014**, *6*, 1485-1498.
14. Pérez-Pérez, M. J.; Priego, E. M.; Bueno, O.; Martins, M. S.; Canela, M. D.;

Liekens, S. Blocking blood flow to solid tumors by destabilizing tubulin: An approach to targeting tumor growth. *J. Med. Chem.* **2016**, *59*, 8685-8711.

15. Singh P.; Anand, A.; Kumar V. Recent developments in biological activities of chalcones: a mini review. *Eur. J. Med. Chem*. **2014**, *85*, 758-777.
16. Li, W.; Sun, H.; Xu, S.; Zhu, Z.; Xu, J. Tubulin inhibitors targeting the colchicine binding site: a perspective of privileged structures. *Future Med. Chem*. **2017**, *9*, 1765-1794.
17. Mirzaei H.; Emami S. Recent advances of cytotoxic chalconoids targeting tubulin polymerization: Synthesis and biological activity. *Eur. J. Med. Chem*. **2016**, *121*, 610-639.
18. Ducki S.; Rennison D.; Woo M.; Kendall A.; Chabert J. F.; McGown A.; Lawrence N. J. Combretastatin-like chalcones as inhibitors of microtubule polymerization. Part 1: synthesis and biological evaluation of antivascular activity. *Bioorg. Med. Chem*. **2009**, *17*, 7698-7710.
19. Lawrence N. J.; Rennison D.; McGown A. T.; Hadfield J. A. The total synthesis of an aurone isolated from Uvaria hamiltonii: aurones and flavones as anticancer agents. *Bioorg. Med. Chem. Lett.* **2003**, *13*, 3759-3763.
20. Romagnoli R.; Baraldi P. G.; Sarkar T.; Carrion M. D.; Cara C. L.; Lopez O. C.; Preti D.; Tabrizi M. A.; Tolomeo M.; Grimaudo S.; Cristina A. D.; Zonta N.; Balzarini J.; Brancale A.; Hsieh H.; Hame E. Synthesis and biological evaluation of 1-methyl-2-(3′, 4′, 5′-trimethoxybenzoyl)-3-aminoindoles as a new class of antimitotic agents and tubulin inhibitors. *J. Med. Chem*. **2008**, *51*, 1464-1468.

21. Ducki S.; Forrest R.; Hadfield J. A.; Kendall, A.; Lawtence N. J.; McGowm A. T.; Rennison D. Potent antimitotic and cell growth inhibitory properties of substituted chalcones. *Bioorg. Med. Chem. Lett*. **1998**, *8*, 1051-1056.

22. Yan J.; Chen J.; Zhang S.; Hu J.; Huang L.; Li X. Synthesis, evaluation, and mechanism study of novel indole-chalcone derivatives exerting effective antitumor activity through microtubule destabilization in vitro and in vivo. *J. Med. Chem.* **2016**, *59*, 5264-5283.

23. Li W.; Yin Y.; Yao H.; Shuai W.; Sun H.; Xu S.; Liu J.; Yao H.; Zhu Z.; Xu J. Discovery of novel vinyl sulfone derivatives as anti-tumor agents with microtubule polymerization inhibitory and vascular disrupting activities. *Eur. J. Med. Chem*. **2018**, *157*, 1068-1080.

24. Álvarez R.; Aramburu L.; Puebla P.; Caballero E.; González M.; Vicente A.; Medarde M.; Peláez R. Pyridine based antitumour compounds acting at the colchicine site. *Curr. Med. Chem*. **2016**, *23*, 1100-1130.

25. Kaur, K.; Jain, M.; Reddy, R. P.; Jain, R. Quinolines and structurally related heterocycles as antimalarials. *Eur. J. Med. Chem*. **2010**, *45*, 3245-3264.

26. Solomon V. R.; Lee H. Quinoline as a privileged scaffold in cancer drug discovery. *Curr. Med. Chem*. **2011**, *18*, 1488-1508.

27. O'Boyle N. M.; Greene L. M.; Keely N. O.; Wang S.; Cotter T. S.; Zisterer M. M.; Meegan M. J. Synthesis and biochemical activities of antiproliferative amino acid and phosphate derivatives of microtubule-disrupting β-lactam combretastatins. *Eur. J. Med. Chem*. **2013**, *62*, 705-721.

28. Pérez-Melero C.; Maya A. B. S.; Rey B. D.; Peláez R.; Caballero E.; Medarde M. A new family of quinoline and quinoxaline analogues of combretastatins. *Bioorg. Med. Chem. Let*. **2004**, *14*, 3771-3774.

29. Chaudhary V.; Venghateri J. B.; Dhaked H. P. S.; Bhoyar A. S.; Guchhait S. K.; Panda D. Novel combretastatin-2-aminoimidazole analogues as potent tubulin assembly inhibitors: exploration of unique pharmacophoric impact of bridging skeleton and aryl moiety. *J. Med. Chem*. **2016**, *59*, 3439-3451.

30. Kasibhatla S.; Baichwal V.; Cai S. X.; Roth B.; Skvortsova I.; Skvortsov S.; Lukas P.; English N. M.; Sirisoma N.; Drewe J.; Pervin.; Tseng B.; Carlson R. O.; Pleiman C. M. MPC-6827: a small-molecule inhibitor of microtubule formation that is not a substrate for multidrug resistance pumps. *Cancer Res*. **2007**, *67*, 5865-5871.

31. Sirisoma N.; Pervin A.; Zhang H.; Jiang S.; Willardsen J. A.; Anderson M. B.; Mather Gary.; Pleiman C. M.; Kasibhatla S.; Tseng B.; Drewe J.; Cai S. Discovery of N-(4-methoxyphenyl)-N,2-dimethylquinazolin-4-amine, a potent apoptosis inducer and efficacious anticancer agent with high blood brain barrier penetration. *J. Med. Chem.* **2009**, *52*, 2341-2351.

32. Wang, X. F.; Wang, S. B.; Ohkoshi, E.; Wang, L. T.; Hamel, E.; Qian, K.; Morris-Natschke, S. L.; Lee, K. H.; Xie, L. N-Aryl-6-methoxy-1,2,3,4-tetrahydroquinolines: A novel class of antitumor agents targeting the colchicine site on tubulin. *Eur. J. Med. Chem.* **2013**, *67*, 196-207.

33. Wang X.; Guan F.; Ohkoshi E.; Guo W.; Wang L.; Zhu D.; Wang S.; Wang L.; Hamel E.; Yang D.; Li L.; Qian K.; Morris-Natschke S. L.; Yuan S.; Lee K.; Xie L. Optimization of 4-(N-cycloamino)phenylquinazolines as a novel class of tubulin-polymerization inhibitors targeting the colchicine site. *J. Med. Chem*. **2014**, *57*, 1390-1402.

34. Banerjee S.; Arnst K. E.; Wang Y.; Kumar G.; Deng S.; Yang L.; Li G.; Yang J.; White S. W. Li W.; Miller D. D. Heterocyclic-Fused pyrimidines as novel tubulin polymerization inhibitors targeting the colchicine binding site: structural basis and antitumor efficacy. *J. Med. Chem*. **2018**, *61*, 1704-1718.

35. Khelifi I.; Naret T.; Renko D.; Hamze A.; Bernadat G.; Bignon J.; Lenoir C.; Dubois J.; Brion J.; Provot O.; Alami M. Design, synthesis and anticancer properties of IsoCombretaQuinolines as potent tubulin assembly inhibitors. *Eur. J. Med. Chem.* **2017**, *127*, 1025-1034.

36. Li W.; Shuai W.; Xu F.; Sun H.; Xu S.; Yao H.; Liu J.; Yao H.; Zhu Z.; Xu J. Discovery of novel 4-arylisochromenes as anticancer agents inhibiting tubulin polymerization. *ACS Med. Chem. Lett*. **2018**, *9*, 974-979.

37. Li W.; Yin, Y.; Shuai W.; Xu F.; Yao H.; Liu J.; Cheng, K.; Xu J.; Zhu Z.; Xu, S. Discovery of novel quinazolines as potential anti-tubulin agents occupying three zones of colchicine domain. *Bioorg. Chem.* **2019**, *83*, 380-390.

38. Patil R.; Patil S. A.; Beaman K. D.; Patil S. A. Indole molecules as inhibitors of tubulin polymerization: potential new anticancer agents, an update (2013–2015). *Future Med. Chem.* **2016**, *8*, 1291-1316.

39. Patil S. A.; Patil R.; Miller D. D. Indole molecules as inhibitors of tubulin polymerization: potential new anticancer agents. *Future Med. Chem*. **2012**, *4*, 2085-2115.

40. Argade A.; Bahekar R.; Desai J.; Thombare P.; Shah K.; Gite S.; Sunder R.; Ranvir R.; Bandyopadhyay D.; Chakrabarti G.; Joharapurkar A.; Mahapatra J.; Chatterjee A.; Patel H.; Shaikh M.; Sairam K. V. V. M.; Jain M.; Patel P. Design, synthesis and biological evaluation of γ-lactam hydroxamate based TACE inhibitors. *MedChemComm* **2011**, *2*, 966-972.

41. Dy, G. K.; Adjei, A. A. Understanding, recognizing, and managing toxicities of targeted anticancer therapies. *Ca-Cancer J. Clin.* **2013**, *63*, 249-279.

42. Gaspari R.; Prota A. E.; Bargsten K.; Cavalli A.; Steinmetz M. O. Structural basis of cis-and trans-combretastatin binding to tubulin. *Chem*. **2017**, *2*, 102-113.

43. Clarke, P. R.; Allan, L. A. Cell-cycle control in the face of damage - a matter of life or death. *Trends Cell Biol.* **2009**, *19*, 89-98.

44. Buolamwini, J. K. Cell cycle molecular targets in novel anticancer drug discovery. *Curr. Pharm. Des*. **2000**, *6*, 379-392.

45. Jordan M. A.; Wilson L. Microtubules and actin filaments: dynamic targets for cancer chemotherapy. *Curr. Opin. Cell Boil.* **1998**, *10*, 123-130.

46. Moldoveanu, T.; Follis, A. V.; Kriwacki, R. W.; Green, D. R. Many players in BCL-2 family affairs. *Trends Biochem. Sci*. **2014**, *39*, 101-111.

47. Sinha, K.; Das, J.; Pal, P. B.; Sil, P. C. Oxidative stress: the mitochondria-dependent and mitochondria-independent pathways of apoptosis.

Arch. Toxicol. **2013**, *87*, 1157-1180.

48. Waris, G.; Ahsan, H. Reactive oxygen species: role in the development of cancer and various chronic condition. *J. Carcinog.* **2006**, *5*, 14.

49. Yamaguchi, H.; Wyckoff, J.; Condeelis J.; Cell migration in tumors. *Curr. Opin. Cell Biol.* **2005**, *17*, 559-564.

50. Friedl, P.; Wolf, K. Tumour-cell invasion and migration: diversity and escape mechanisms. *Nat. Rev. Cancer*. **2003**, *3*, 362-374.

51. Schwartz, E. L. Antivascular actions of microtubule-binding drugs. *Clin. Cancer Res.* **2009**, *15*, 2594-2601.

52. Lamalice L.; Boeuf F. L.; Huot J. Endothelial cell migration during angiogenesis. *Circ. Res.* **2007**, *100*, 782-794.

53. Lamaa, D.; Lin, H.; Zig, L.; Bauvais, C.; Bollot, G.; Bignon, J.; Levaique, H.; Pamlard, O.; Dubois, J.; Ouaissi, M.; Souce, M.; Kasselouri, A.; Saller, F.; Borgel, D.; Jayat-Vignoles C.; Al-Mouhammad, H.; Feuillard, J.; Benihoud, K.; Alami, M.; Hamze, A. Design and synthesis of tubulin and histone deacetylase inhibitor based on iso-combretastatin A‑4. *J. Med. Chem.* **2018**, *61*, 6574-6591.

54. Gross, G.; Tardio, J.; Kuhlmann, O. Solubility and stability of dalcetrapib in vehicles and biological media. *Int. J. Pharm*. **2012**, *437*, 103-109.

55. Chen, J.; Wang, Z.; Li, C. M.; Lu, Y.; Vaddady, P. K.; B. Meibohm, J.T. Dalton, D.D. Miller, W. Li, Discovery of novel 2-aryl-4-benzoyl-imidazoles targeting the colchicines binding site in tubulin as potential anticancer agents, *J. Med. Chem*. **2010**, *53*, 7414-7427.

56. Bonacorso H. G.; Nogara P. A.; Silva F.; Rosa W. C.; Wiethan C. W.; Zanatta N.; Martins M. A. P.; Rocha J. B. T. Convergent synthesis and cytotoxicity of novel trifluoromethyl-substituted (1H-pyrazol-1-yl)(quinolin-4-yl) methanones. *J. Fluorine. Chem*. **2016**, *190*, 31-40.

Table of Contents Graphic

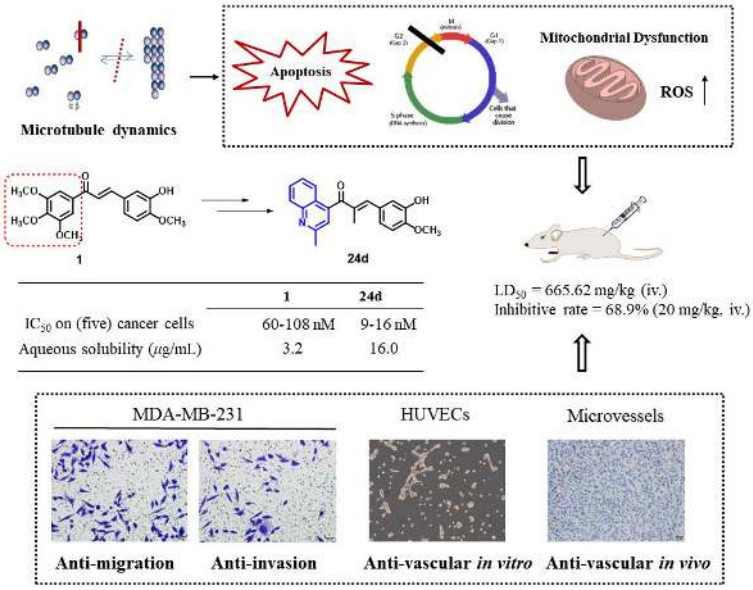

	1	24d
IC_{50} on (five) cancer cells	60-108 nM	9-16 nM
Aqueous solubility (μg/mL)	3.2	16.0